International Journal of
Molecular Sciences

MDPI

Article

Musashi-1: An Example of How Polyalanine Tracts Contribute to Self-Association in the Intrinsically Disordered Regions of RNA-Binding Proteins

Tsai-Chen Chen [1] and Jie-rong Huang [1,2,*]

[1] Institute of Biochemistry and Molecular Biology, National Yang-Ming University, No. 155 Section 2 Li-nong Street, Taipei 11221, Taiwan; hazelnut.chen.scu@gmail.com
[2] Institute of Biomedical Informatics, National Yang-Ming University, No. 155 Section 2 Li-nong Street, Taipei 11221, Taiwan
* Correspondence: jierongh@ym.edu.tw

Received: 3 March 2020; Accepted: 24 March 2020; Published: 26 March 2020

Abstract: RNA-binding proteins (RBPs) have intrinsically disordered regions (IDRs) whose biophysical properties have yet to be explored to the same extent as those of the folded RNA interacting domains. These IDRs are essential to the formation of biomolecular condensates, such as stress and RNA granules, but dysregulated assembly can be pathological. Because of their structural heterogeneity, IDRs are best studied by NMR spectroscopy. In this study, we used NMR spectroscopy to investigate the structural propensity and self-association of the IDR of the RBP Musashi-1. We identified two transient α-helical regions (residues ~208–218 and ~270–284 in the IDR, the latter with a polyalanine tract). Strong NMR line broadening in these regions and circular dichroism and micrography data suggest that the two α-helical elements and the hydrophobic residues in between may contribute to the formation of oligomers found in stress granules and implicated in Alzheimer's disease. Bioinformatics analysis suggests that polyalanine stretches in the IDRs of RBPs may have evolved to promote RBP assembly.

Keywords: RNA-binding proteins; intrinsically disordered proteins; polyalanine; liquid–liquid phase separation; self-association

1. Introduction

The human genome encodes more than 1500 RNA-binding proteins (RBPs) [1]. In addition to canonical RNA-binding domains, most, if not all, RBPs have intrinsically disordered regions (IDRs) [2–5], whose importance has only recently come to light [6,7]. Pioneering studies have shown that some RBPs (including FUS, hnRNPA1, hnRNPA2 and TIA1) use their IDRs to form "dynamic fibers" that may play a role in organizing membraneless cellular structures, such as RNA granules and stress granules [8]. Another function mediated by IDRs is liquid–liquid phase separation (LLPS), which has recently been shown to govern the coordination of cellular membraneless organelles [9,10]. RBPs are the protein family whose IDR-mediated LLPS has been the most studied, notably in terms of the effect of mutations on functional assembly and pathological aggregation [11,12], interactions with other molecules that disrupt or promote self-assembly [13,14], posttranslational modification effects [15,16], residues or sequence motifs that promote condensation [17,18], and their regulation in alternative splicing [19,20]. In spite of the growing literature on these IDRs, residue-specific information, which would provide crucial functional insights, is available for just a few members [21–24] of this 1500+ family. More structural studies of these IDRs are required to improve our understanding and deduce family-wide rules.

Musashi-1 is a particularly interesting RBP. Its roles in mediating stem cell regeneration and cell differentiation are well-known [25], and recent evidence suggests it may be implicated in neurodegenerative diseases [26,27], as have the prominent RBPs TDP-43 and FUS [28,29]. The removal of Musashi-1's IDR prevents this protein's recruitment to stress granules that reduce the chemoresistance of some types of cancer cells [30,31]. This role in granule formation resembles those of other neurodegeneration-associated RBPs; for example, FUS forms liquid-like compartments under stress that recruit proteins to repair damaged DNA, but can also transition to a fibrous, pathological state [11]; likewise, hnRNPA1 acts as a scaffold for stress granules, but this can also lead to pathological aggregation [12].

Musashi-1's IDR differs in its primary sequence from many of those that have been studied to date. Although its RNA recognition motifs (as predicted by PROSITE [32] and in experimentally solved structures [33,34]) and low sequence complexity (predicted by the SEG algorithm [35]) are similar to those of other known RBPs, the levels of structural disorder predicted for the C-terminal part (residues 194–362; Figure 1A,B) vary depending on the algorithm used. This is probably because of the predominance of hydrophobic residues and the low proportion of charged residues (Figure 1C,D), which are features of folded proteins—as also shown by FoldIndex predictions [36] and its location in the charge-hydropathy plot (Figure 1E,G). Unlike other RBPs implicated in neurodegenerative diseases (see Supplementary Figure S1 for examples), it is not prion-like (Figure 1F). Another unusual feature of its primary sequence is the presence of a polyalanine tract (eight consecutive alanines) in the center, and contrary to the IDRs of many other RBPs [4,5], there are no SR-repeats, RG/RGG motifs, Q/N-rich stretches, or [G/S]Y[G/S] motifs (Figure 1H). How this unique sequence is involved in neurodegenerative disease and/or stress granule recruitment are questions that remain to be answered. In this study, we used NMR spectroscopy to obtain residue-specific information on the IDR, revealing two parts with α-helical propensity. In combination with circular dichroism (CD) and micrography data, the NMR results suggest that the helices are involved in self-association. More generally, the fact that one of the helices in the polyalanine stretch is also found in many other RBPs suggests that polyalanine tracts may have evolved as a means of self-assembly.

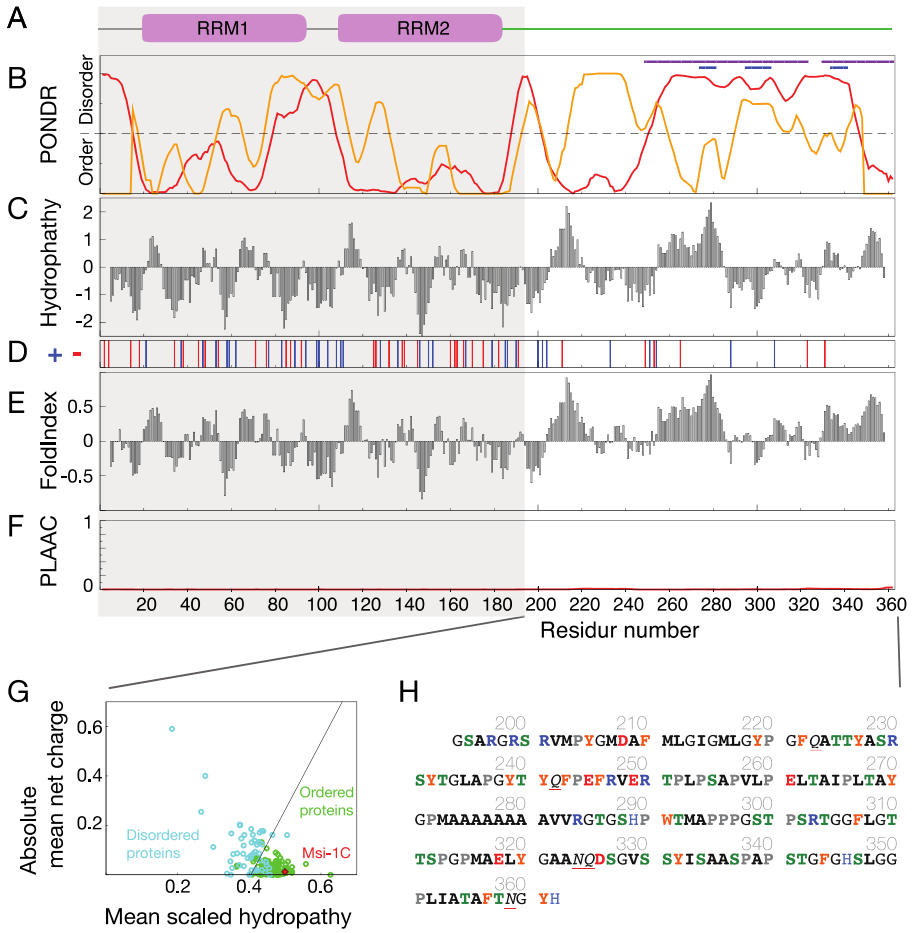

Figure 1. Primary sequence analysis of Musashi-1. (**A**) Functional domains predicted by PROSITE [32] and deposited structures. (**B**) Levels of protein disorder predicted by the PONDR VLXT (red) and XL1_XT (yellow) algorithms [37]. The two regions with low sequence complexity predicted using the SEG algorithm [35] are shown with blue and purple bars. (**C**) Hydropathy according to the Kyte and Doolitte scale (average window size: 9). The scale of each amino acid is derived from experimental observations from solved structures [38]. (**D**) Positions of positively (blue) and negatively (red) charged residues. (**E**) FoldIndex folding [36]. (**F**) Prion-likeness predicted by the PLAAC algorithm [39]. (**G**) Charge–hydropathy plot for a database of known disordered proteins (blue) and folded proteins (green) and the residues 194–362 of Musashi-1 (red) [37]. (**H**) The primary sequence used in this study, with residues labeled according to their properties (blue: positive; red: negative; green: potential phosphorylation sites; orange: aromatic residues; gray: prolines; black: hydrophobic residues).

2. Results and Discussion

2.1. Chemical Shift Assignment of Musashi-1

The chemical shift assignments for the IDRs of Musashi-1 (residues 194–362; BMRB access number: 50204) are shown in Figure 2A (pH 5.5, 283 K). The protein is prone to aggregation and proline-rich (~12% in the sequence), so a specific assignment strategy was used, as described in the Material and Methods section and the Supplementary Information. Although the PASTA algorithm [40] predicts four α-helices based on the primary sequence (Figure 2B), secondary chemical shift analysis indicates that just two regions, residues ~208–218 and ~270–284, form transient α-helices (Figure 2C–E), with populations (predicted using the δ2D algorithm [41] derived from the molecular dynamics simulation and experimental observations of conformational equilibrium of multiple states, using Cα, Cβ, C′, HN, and NH chemical shifts) of 28% and 45% at most (Figure 2F).

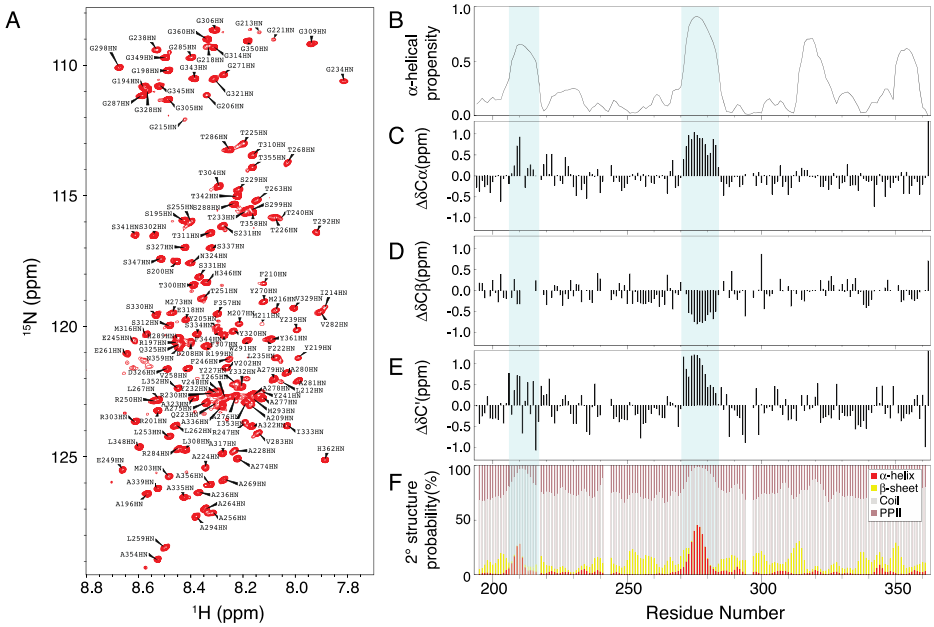

Figure 2. NMR chemical shift assignment of Musashi-1. (**A**) HSQC spectrum of Musashi-1 at 283 K and pH 5.5 with peak assignments. Except L217, Q242, F243, and L319, all non-proline peaks are assigned. (**B**) Residue-specific α-helical propensities predicted using the PASTA program. (**C–E**) Secondary chemical shifts for Cα (**C**), Cβ (**D**), and C′ (**E**) atoms. (**F**) Stacked plot of secondary structure probability based on the assigned chemical shifts, calculated using the δ2D algorithm (red: α-helix; yellow: β-sheet; gray: random coil; brown: polyproline II helix).

2.2. Musashi-1 Self-Association

The implication of Musashi-1 in neurodegenerative diseases and the role of its IDR in stress granule recruitment [30,31] suggest that it has a propensity to self-assemble as observed in many RBPs [11,12,23]. The HSQC spectra measured for 20 and 100 μM protein samples at pH 5.5, under different temperatures (Figure 3A), show decreased intensities in the N-terminal region, between the two α-helical elements. Many of the peaks in the HSQC spectra have distorted line shapes, notably those from residues in between and within the two helical stretches, because of the kinetics among many conformations (monomer and oligomer) in the intermediate exchange regime (Figure 3B; representative peaks that are not distorted or broadened are shown in Supplementary Figure S2). The peak intensity ratios between the two protein concentrations are less than the corresponding molar ratio (Figure 3C). Furthermore, the average intensity ratio is lower at higher temperatures (3.51, 3.17, and 2.05 at 283, 293, and 303 K, respectively, compared with a molar ratio of 5). At 283K, the intensity ratios in the first α-helical region are even lower, suggesting that the dynamics of this region are reduced at higher concentrations because of stronger self-association. This is not observed at the other two temperatures, because higher temperatures promote the formation of NMR-invisible oligomers at the higher concentration, which reduce the intensity ratio uniformly for all residues, thereby masking the residue-specific soluble monomer/multimer equilibrium effect. Micrographs of the oligomers that form at 293 and 303 K are shown in Figure 3D. The oligomers do not disappear when the temperature is reduced, and as a result, once the samples were heated to 303 K, the NMR intensity remained low when the temperature was decreased back to 283 K (Supplementary Figure S3). SDS-PAGE data confirm that this was not because of protein degradation (Figure 3E). The fact that the transverse relaxation rate constants (R_2) are similar for these two concentrations at all temperatures suggests that the concentration-related decrease in intensity is unlikely due to chemical exchange (e.g., a monomer–oligomer equilibrium; Figure 3F), and confirm that the reduced NMR intensity at higher temperatures is due to the formation of oligomers. Figure 3G shows the CD spectra of 20 μM

samples recorded at different temperatures. The α-helical propensities estimated using the BeStSel algorithm [42,43] are 6.0 ± 1.3% at 283 K and 9.4 ± 0.5% at 303 K (Figure 3G inset). This increase in α-helical population may be sufficient to form the oligomers observed micrographically (Figure 3D).

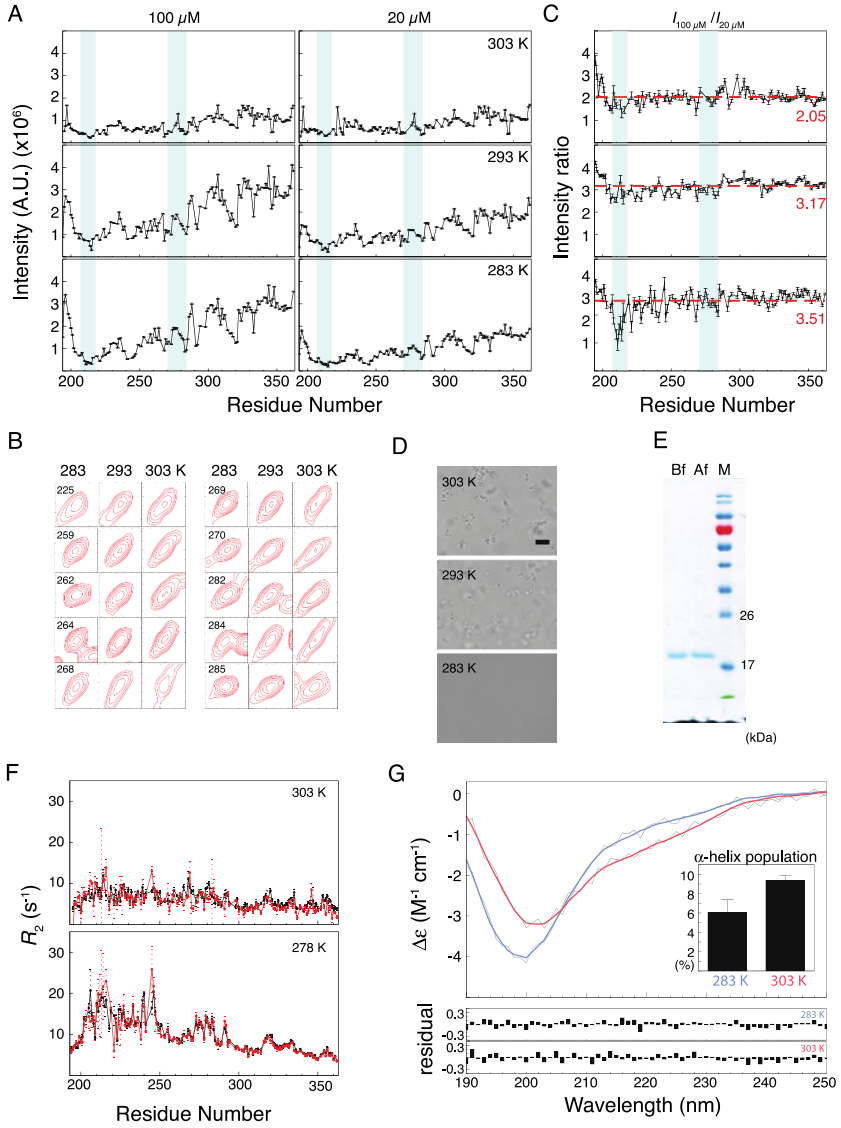

Figure 3. Temperature and concentration dependence of Musashi-1 oligomerization. (**A**) NMR HSQC peak intensities measured at two concentrations (100 and 20 μM) and three temperatures (283, 293, and 303 K) at pH 5.5. Regions with α-helical propensity are shaded blue. (**B**) Selected peaks showing evidence of line-broadening with increasing temperature. The residue number is indicated on the left-upper corner in each panel. (**C**) Peak intensity ratios between 100 and 20 μM samples. The numbers (red) indicate the averaged values. (**D**) Micrographs of the oligomers formed at 293 and 303 K (scale bar = 10 μm) of 20 μM samples. (**E**) SDS-PAGE analysis of protein integrity before (Bf) and after (Af) having increased the temperature above the oligomerization threshold. (**F**) Transverse relaxation rate constants (R_2) at 278 and 303 K for 20 μM (red) and 100 μM (black) samples. (**G**) Circular dichroism spectra for 20 μM samples (pH 5.5) at 283 K (blue) and 303 K (red) fitted using the BeStSel algorithm (gray lines: raw data). The inset compares the average α-helical populations at the two temperatures (three repeats; mean ± SD). Fitting residuals are shown in the lower panel.

2.3. Formation of Musashi-1 Oligomers in a Time-Dependent Manner and at a Higher pH

Figure 4A illustrates how the NMR peak intensities decreased over time: by more than 80% overall after 24 h for the 100 μM sample. SDS-PAGE shows that this is not because of sample degradation (Figure 4B). The NMR signal intensity also decreased overall on increasing the pH of the sample to 5.7 or 6 (Figure 4C), again, not because of protein degradation (Figure 4D). These results suggest that increasing the pH alters the balance between electrostatic repulsion (from the net positive charge (+2) of the IDR) and hydrophobic attraction in favor of the latter, leading to oligomerization. Similar assembly behavior was observed by using microscopy after longer incubation times at pH 5.5 or a freshly prepared sample at pH 6 (Figure 4E,F). No fluorescence signals were observed in ThT assays, indicating that there are no cross-beta structures in the oligomers (Figure 4G). (Note that fluorescence signals from cross-beta structures were observed in control ThT assays performed on the C-terminal ID domain of TDP-43). The precipitation of the protein made it difficult to use CD spectroscopy to estimate its secondary structure, as the Δε values (Equation (1)) used as input for the program became more uncertain as aggregates formed and the signal intensity decreased.

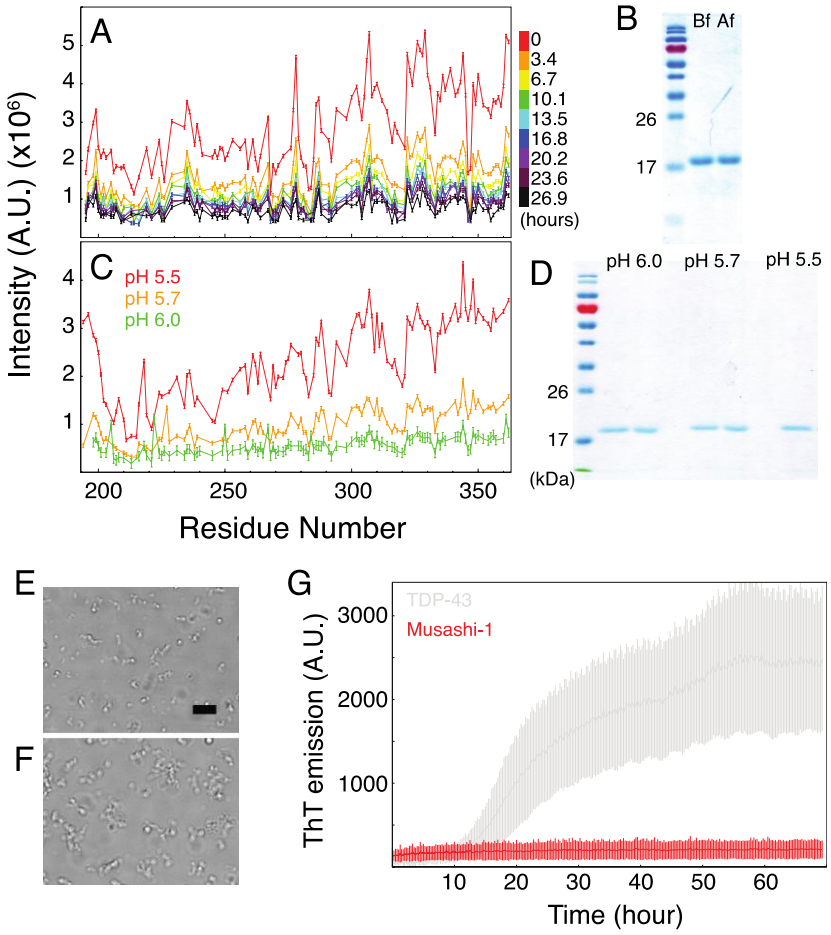

Figure 4. Analysis of the non-cross-beta Musashi-1 oligomers formed at lower pHs and after prolonged incubation. (**A**) Decrease in NMR HSQC peak intensity as a function of time. Data collected at 303 K, pH 5.5. (**B**) SDS-PAGE analysis of protein integrity before (Bf) and after (Af) the one-day NMR experiments, whose results are shown in panel A. (**C**) NMR HSQC peak intensities at 283 K and pH 5.5, 5.7, and 6.0 and 283 K. (**D**) SDS-PAGE analyses of the samples prepared at pH 5.5, 5.7, and 6.0. (**E,F**) Micrographs of samples (**E**) incubated at 303 K for 24 h at pH 5.5 or (**F**) freshly prepared at pH 6. Scale bar = 10 μm. (**G**) ThT assay of Musashi-1 (red) and the C-terminal domain of TDP-43 (control experiment; gray).

2.4. The Role of Polyalanine Tracts in Musashi-1 and in RBPs in General

The structured RNA recognition domains of RBPs have binding pockets that have evolved to identify specific nucleic acids sequences. However, how RBPs are recruited to the gene-regulation machinery remains largely unknown. Most RBPs have IDRs whose role in controlling the entire proteins' location has only recently come to light. The features of these IDRs, including [G/S]-[F/Y/W]-[G/S] motifs [17,44], cation-π interactions [16,18], charge–charge interactions [45], and prion-like behavior [46], lead them to assemble in response to environmental changes. Polyalanine tracts may play a similar role in the regulation of RBP assembly, as shown here for Musashi-1. Polyalanine tracts have been implicated in many diseases [47] and can act as nuclear export signals [48]. The assembly of polyalanine stretches into α-helical clusters without forming amyloid-fibrils has also been demonstrated in both model peptides and proteins with polyalanine tracts [49]. Recent studies on aggregation-prone proteins and those with prion-like domains have shown that forming higher-order oligomers is their physiological role, albeit at the price of pathological aggregation, when the process is perturbed [50]. The same reasoning can be applied to polyalanine tracts, in the sense that, although they can induce the formation of oligomers that in turn promote amyloid formation [49], they may also have physiologically important roles in the formation of higher-order assemblies.

Among the 20,000+ human protein sequences in the UniProtKB/Swiss-Prot database, gene ontology (GO) annotations indicate that about 20.3% (listed in the Supporting Information) are RNA-related (including RNA polymerases associated functions), and 7.7% are specifically related to "RNA binding". The proportion of proteins with polyalanine tracts (5–20 repeats) that are RNA-related is much higher; for example, more than 60% of those with 7–16 repeats are associated to RNA-related function. Only considering proteins tagged as "RNA binding", the proportion of proteins with stretches of 5–10 alanine repeats can be twice as high as in the database as a whole (Figure 5A; Supplementary Table S2). There is, therefore, an association between the presence of polyalanine tracts and RNA-related function.

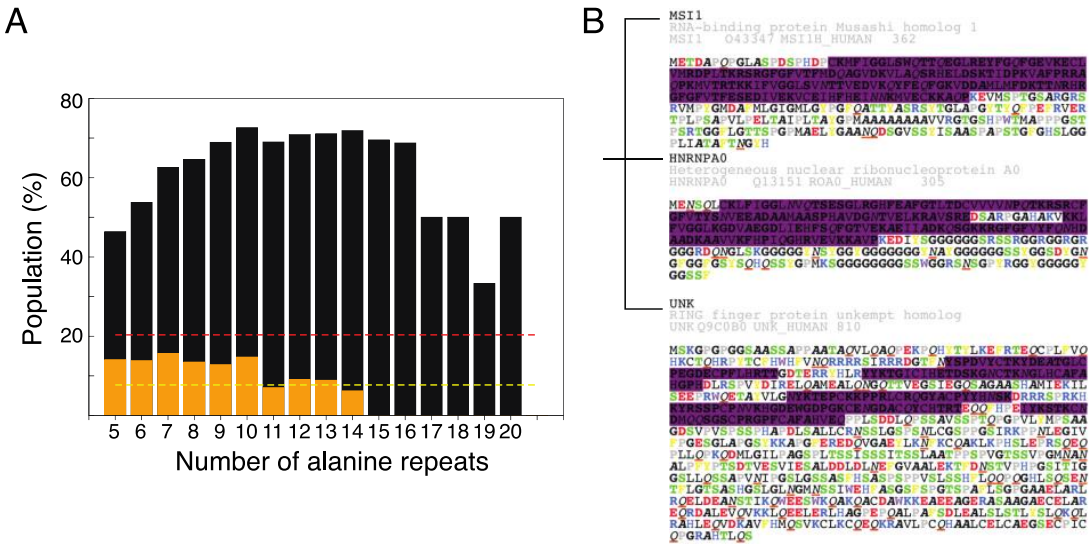

Figure 5. Polyalanine tracts are a common feature of RNA related proteins, and may be one of the ways in which RBPs self-assemble through their IDRs. (**A**) Bioinformatics analysis of the proportions of human proteins with different lengths of alanine repeats (from 5 to 20) either related to RNA function (black bars; the red dashed line shows the proportion overall) or specifically labeled "RNA binding" (orange bars; overall proportion, yellow dashed line). (**B**) Illustration of the differences in the IDRs of RBPs that bind to similar RNA motifs. The purple shaded regions are those identified by PROSITE as RNA recognition motifs. The amino acids are colored according to their physical properties (positive charge: blue; negative charge: red; F/Y: yellow; W: purple; S/T (potential phosphorylation site for the addition of negative charges): green; P: gray; A: italic-bold black; Q/N: red underlined italic).

In a recent study [51], Dominguez et al. purified the RNA recognition domains of a representative group of RBPs, identified their interacting RNA motifs, and then hierarchically clustered the RBPs in terms of their RNA-binding motifs. Roughly a quarter of these RBPs (18 out of 76) have polyalanine tracts ranging from 5 to 13 repeats (Supplementary Table S3), in agreement with our hypothesis that polyalanine tracts are one of the many features of RBP IDRs. More importantly, while those RBPs bind to similar RNA motifs, the physicochemical properties of their disordered regions have little in common. For example, the polyalanine feature of Musashi-1 (see Reference [51]) is not found in the IDRs from the same groups of RBPs that binds similar RNA-motif: UNK (which has charged blocks) or hnRNPA0 (which has G/S-F/Y/W-G/S motifs; Figure 5B), and there are other examples in other RNA-motif groups (Supplementary Figure S4). Even though some RBPs have similar RNA-binding motifs, their IDRs may have evolved different physical properties that ensure specific spatiotemporal regulation.

This focus on continuous polyalanine tracts may be too restrictive, and the above analysis may have underestimated the importance of α-helix. Many other types of amino acids can form α-helices, and many polyalanine tracts in the database are non-continuous. For example, the IDR of TDP-43 has a transient α-helical region [23] (primary sequence, AMMAAAQAA) that is involved in self-association. Furthermore, a disrupted polyalanine tract may still contribute to self-assembly in combination with a few [G/S]-[F/Y/W]-[G/S] motifs or an increased prion-like propensity (Supplementary Figure S1).

3. Material and Methods

3.1. Musashi-1 Primary Sequence Analysis

The primary sequence of full-length Musashi-1 was taken from the UniProt database (entry number O43347) and used as input for the programs PROSITE [32], PONDR [37], ProtScale [52], FoldIndex [36], PLAAC [39], and PASTA [40], to predict the properties of the protein.

3.2. Polyalanine Tracts Analysis

The UniProt Knowledgebase of manually curated human protein information (UniProtKB/Swiss-Prot, entries for 20367 human proteins as of 8 January 2020) was downloaded from the UniProt website [53]. Proteins with different lengths of polyalanine tracts were extracted, using the "Peptide search" function on the same website. Proteins with RNA-related keywords in gene ontology annotations were counted, using an in-house script.

3.3. DNA Construct

The cDNA of Musashi-1 was provided by Dr. Wei-Yi Chen (NYMU). The C-terminal domain (residue numbers 194 to 362) was cloned to a pET-21 vector, using *NdeI* and *XhoI* restriction enzymes. A hexa-histidine tag was added to the N-terminus for purification. No further non-native residues were added. To assist NMR assignment, four constructs with deleted fragments were prepared, using the primers listed in Supplementary Table S1. All constructs were fully sequenced.

3.4. Protein Expression and Purification

Single colonies of transformed *E. coli.* BL21 (DE3) or Rosetta were selected from an ampicillin agar plate and used to inoculate 5.0 mL of lysogeny broth containing 0.1 mg·mL^{-1} ampicillin. The pre-culture was left in a 37 °C shaker, overnight, and used to inoculate 500 mL of lysogeny broth or minimal M9 medium (containing $^{15}NH_4Cl$ and/or ^{13}C-glucose for isotope labeling). The growth cultures were left in a 37 °C shaker and shaken vigorously until the $O.D_{600}$ reached 0.6. The cells were induced with a final concentration of 1 mM isopropyl β-D-1-thiogalactopyranoside and left shaking at 25 °C, overnight. The harvested cells were lysed by sonication in 20 mM Tris buffer at pH 8. After centrifugation (Beckman JA25.5, 30 min, 18,000 rpm, at 4 °C), the inclusion bodies were dissolved with the same lysis buffer, with an additional 8 M urea. After the second centrifugation (10,000 rpm, 30 min), the supernatant was passed through a 0.45 μm filter and loaded onto a nickel-charged immobilized

metal-ion affinity chromatography column (Qiagen, Hilden, Germany). The column was washed with ten volumes of 20 mM Tris buffer with 8 M urea at pH 8 to remove non-specific binding proteins. The target protein was eluted with an additional 500 mM imidazole in the same wash buffer. The eluted sample was acidified, using trifluoroacetic acid, to a pH lower than 3, and then loaded into a C4 reverse-phase column (Thermo Scientific Inc., MA, USA). The protein was eluted with an increasing gradient of acetonitrile mixed with triple-distilled water, using an HPLC system. The eluted sample was immediately frozen with liquid nitrogen and lyophilized. The lyophilized sample was stored in a drying cabinet, until use.

3.5. Chemical Shift Assignment

The assignment experiments were performed on a Bruker AVANCE 800 MHz spectrometer, at 283 K. A denaturation-then-titration strategy (assigning the protein under harsh conditions and then titrating to physiological conditions; see Supplementary Information) was used to assign the chemical shifts of the protein. In addition to standard pulse sequences (HNCO, HN(CA)CO, HNCA, HN(CO)CA, HNCACB, and CBCA(CO)NH), we also used (H)N(COCO)NH and (HN)CO(CO)NH [54] to complete the sequential assignments of long-range (i, i+2) backbone nitrogen and carbonyl carbon atoms separated by prolines. Different fragments were created to confirm the assignment (see Supplementary Information). Secondary chemical shifts were analyzed by using Kjaergaard et al.'s database of random coil shifts [55]. Secondary structure probabilities based on the chemical shifts were calculated by using the δ2D program [41].

3.6. NMR Experiments and Analysis

The urea and pH titration experiments were monitored, using HSQC spectra [56] (with WATERGATE [57] solvent suppression) recorded on Bruker AVANCE III 600 and 850 MHz spectrometers. All the samples were freshly prepared: The estimated amount of lyophilized sample required was dissolved in 20 mM MES buffer with protease inhibitor cocktail (Roche, Basel,, Switzerland); the samples were centrifuged at 12,000× g for 5 min, to remove any aggregates; and the concentration was confirmed by measuring the absorbance at 280 nm on a NanoDrop spectrometer (Thermo Scientific Inc., MA, USA). Transverse relaxation rate constants were measured on the 850 MHz spectrometer, using standard pulse sequences [58] (with delays of 17.2, 34.3, 51.5, 68.6, 120.1, and 154.4 ms). Peak intensities were fitted to exponential decays with a Monte Carlo procedure, to estimate fitting error. All dynamics data were collected in an interleaved manner, with an inter scan delay of 3 s.

3.7. Circular Dichroism Spectroscopy

Circular dichroism spectra were recorded by using an AVIV model 410 spectropolarimeter. A 0.1 mm cuvette was used. Data were collected between 190 and 260 nm, with an interval of 1 nm. Ten measurements were co-added for each data point, and all the experiments were performed in triplicate. The measured theta machine units (θ) were converted to $\Delta\varepsilon$, using the following equation [59]:

$$\Delta\varepsilon = \theta \times \frac{0.1 \times MRW}{l \times C \times 3298} \quad (1)$$

where MRW is the mean residue weight (molecular weight/residue number, in Dalton), l is the path length (in cm), and C is the protein concentration (in mg/mL). The resulting curves were fitted, using the program BeStSel [42,43], to estimate secondary structure populations. Samples (20 μM) were prepared in 20 mM MES buffer at pH 5.5, at different temperatures, otherwise indicated.

3.8. Microscopy

Micrographs were collected by using an Olympus BX51 device with a 40× long working-distance objective lens, and the images were recorded with a Zeiss AxioCam MRm camera. The samples were placed on a thermostatic microscope stage (THM120, Linkam Scientific Inc., Tadworth, U.K.) and were equilibrated for 5 min, before collecting the images.

3.9. Thioflavin T Fluorescence Assay

A 1 M stock solution of Thioflavin T (ThT, Acros organics) was prepared in 90% (*v*/*v*) ethanol and protected from light prior to use. The ThT stock was diluted, using 20 mM MES-NaOH buffer to obtain a 1 mM ThT working solution. Protein sample solutions were mixed with the ThT working solution to the designed final concentration. Each sample (120 µL) was distributed in a black 96-well plate. The plates were sealed and transferred to an Infinite 200 (TECAN) multimode microplate reader and incubated at 30 °C. The emission intensity at 480 nm was recorded, using slit widths of 5 nm for both excitation and emission. At least three independent experiments were performed for each condition.

4. Conclusions

While developments in cryogenic electron microscopy [60–63] have revolutionized structural biology [64], NMR spectroscopy remains the most powerful tools to study protein dynamics, especially IDRs and IDPs, with residue-specific resolution [65]. RNA-binding proteins are a large family of proteins with high sequence variability in their IDRs. This study of Musashi-1 illustrates the power of NMR spectroscopy to study disordered proteins. The assignment strategy we used can be applied to many other aggregation-prone proteins, and the chemical shift assignments here can be used to conduct further studies of how its IDRs interact with binding partners [66,67]. Indeed, some identified interacting regions cover the first α-helix, which might be critical for their interaction [66,67]. Our results highlight Musashi-1's ability to self-assemble through interactions involving the region between the two α-helical elements. They also provide a mechanistic explanation of how this protein forms pathological oligomers and is recruited into stress granules via its polyalanine tracts. Polyalanine tracts are found in the IDRs of many other RBPs, suggesting that they have evolved as a means to control where and when RBPs self-assemble.

Accession Numbers: The backbone chemical shift assignments of Musashi-1 were deposited in the BMRB, under accession code 50204.

Supplementary Materials: Supplementary materials can be found at http://www.mdpi.com/1422-0067/21/7/2289/s1.

Author Contributions: Conceptualization, J.-r.H.; validation, T.-C.C. and J.-r.H.; formal analysis, T.-C.C. and J.-r.H.; investigation, T.-C.C. and J.-r.H.; data curation, T.-C.C. and J.-r.H.; writing, J.-r.H.; supervision, J.-r.H; funding acquisition, J.-r.H. All authors have read and agreed to the published version of the manuscript.

Funding: This research was funded by the Ministry of Science and Technology of Taiwan, grant numbers 106-2113-M-010-005-MY2 and 108-2113-M-010-005. The APC was funded by the Ministry of Science and Technology of Taiwan.

Acknowledgments: The authors thank Prof. Won-Jing Wang (NYMU) for access to the microscope, Academia Sinica High-Field NMR Center (HFNMRC) for technical support (HFNMRC is funded by Academia Sinica Core Facility and Innovative Instrument Project (AS-CFII-108-112)), the Instrumentation Centre in National Taiwan University for access to NMR spectrometers, Dr. Shing-Jong Huang (NTU) for help setting up NMR assignment experiments, and Ting Wang for initial work on this project.

Conflicts of Interest: The authors declare no conflict of interest. The funders had no role in the design of the study; in the collection, analyses, or interpretation of data; in the writing of the manuscript; or in the decision to publish the results.

Abbreviations

RBP	RNA-binding proteins
IDP	Intrinsically disordered proteins
NMR	Nuclear magnetic resonance
CD	Circular dichroism
HSQC	Heteronuclear single-quantum coherence
SDS-PAGE	Sodium dodecyl sulfate–polyacrylamide gel electrophoresis

References

1. Gerstberger, S.; Hafner, M.; Tuschl, T. A census of human RNA-binding proteins. *Nat. Rev. Genet.* **2014**, *15*, 829–845. [CrossRef] [PubMed]
2. Varadi, M.; Zsolyomi, F.; Guharoy, M.; Tompa, P. Functional Advantages of Conserved Intrinsic Disorder in RNA-Binding Proteins. *PLoS ONE* **2015**, *10*, e0139731. [CrossRef]
3. Zagrovic, B.; Bartonek, L.; Polyansky, A.A. RNA-protein interactions in an unstructured context. *FEBS Lett.* **2018**, *592*, 2901–2916. [CrossRef] [PubMed]
4. Calabretta, S.; Richard, S. Emerging Roles of Disordered Sequences in RNA-Binding Proteins. *Trends Biochem. Sci.* **2015**, *40*, 662–672. [CrossRef]
5. Jarvelin, A.I.; Noerenberg, M.; Davis, I.; Castello, A. The new (dis)order in RNA regulation. *Cell Commun. Signal.* **2016**, *14*, 9. [CrossRef] [PubMed]
6. Daubner, G.M.; Clery, A.; Allain, F.H. RRM-RNA recognition: NMR or crystallography... and new findings. *Curr. Opin. Struct. Biol.* **2013**, *23*, 100–108. [CrossRef] [PubMed]
7. Leitner, A.; Dorn, G.; Allain, F.H. Combining Mass Spectrometry (MS) and Nuclear Magnetic Resonance (NMR) Spectroscopy for Integrative Structural Biology of Protein-RNA Complexes. *Cold Spring Harb. Perspect. Biol.* **2019**, *11*, a032359. [CrossRef] [PubMed]
8. Kato, M.; Han, T.W.; Xie, S.; Shi, K.; Du, X.; Wu, L.C.; Mirzaei, H.; Goldsmith, E.J.; Longgood, J.; Pei, J.; et al. Cell-free formation of RNA granules: Low complexity sequence domains form dynamic fibers within hydrogels. *Cell* **2012**, *149*, 753–767. [CrossRef]
9. Alberti, S.; Gladfelter, A.; Mittag, T. Considerations and Challenges in Studying Liquid-Liquid Phase Separation and Biomolecular Condensates. *Cell* **2019**, *176*, 419–434. [CrossRef]
10. Banani, S.F.; Lee, H.O.; Hyman, A.A.; Rosen, M.K. Biomolecular condensates: Organizers of cellular biochemistry. *Nat. Rev. Mol. Cell Biol.* **2017**, *18*, 285–298. [CrossRef]
11. Patel, A.; Lee, H.O.; Jawerth, L.; Maharana, S.; Jahnel, M.; Hein, M.Y.; Stoynov, S.; Mahamid, J.; Saha, S.; Franzmann, T.M.; et al. A Liquid-to-Solid Phase Transition of the ALS Protein FUS Accelerated by Disease Mutation. *Cell* **2015**, *162*, 1066–1077. [CrossRef] [PubMed]
12. Molliex, A.; Temirov, J.; Lee, J.; Coughlin, M.; Kanagaraj, A.P.; Kim, H.J.; Mittag, T.; Taylor, J.P. Phase separation by low complexity domains promotes stress granule assembly and drives pathological fibrillization. *Cell* **2015**, *163*, 123–133. [CrossRef] [PubMed]
13. Yoshizawa, T.; Ali, R.; Jiou, J.; Fung, H.Y.; Burke, K.A.; Kim, S.J.; Lin, Y.; Peeples, W.B.; Saltzberg, D.; Soniat, M.; et al. Nuclear Import Receptor Inhibits Phase Separation of FUS through Binding to Multiple Sites. *Cell* **2018**, *173*, 693–705.e22. [CrossRef] [PubMed]
14. Guo, L.; Kim, H.J.; Wang, H.; Monaghan, J.; Freyermuth, F.; Sung, J.C.; O'Donovan, K.; Fare, C.M.; Diaz, Z.; Singh, N.; et al. Nuclear-Import Receptors Reverse Aberrant Phase Transitions of RNA-Binding Proteins with Prion-like Domains. *Cell* **2018**, *173*, 677–692.e20. [CrossRef]
15. Hofweber, M.; Hutten, S.; Bourgeois, B.; Spreitzer, E.; Niedner-Boblenz, A.; Schifferer, M.; Ruepp, M.D.; Simons, M.; Niessing, D.; Madl, T.; et al. Phase Separation of FUS Is Suppressed by Its Nuclear Import Receptor and Arginine Methylation. *Cell* **2018**, *173*, 706–719.e13. [CrossRef]
16. Qamar, S.; Wang, G.; Randle, S.J.; Ruggeri, F.S.; Varela, J.A.; Lin, J.Q.; Phillips, E.C.; Miyashita, A.; Williams, D.; Ströhl, F.; et al. FUS Phase Separation Is Modulated by a Molecular Chaperone and Methylation of Arginine Cation-pi Interactions. *Cell* **2018**, *173*, 720–734.e15. [CrossRef]
17. Lin, Y.; Currie, S.L.; Rosen, M.K. Intrinsically disordered sequences enable modulation of protein phase separation through distributed tyrosine motifs. *J. Biol. Chem.* **2017**, *292*, 19110–19120. [CrossRef]

18. Wang, J.; Choi, J.M.; Holehouse, A.S.; Lee, H.O.; Zhang, X.; Jahnel, M.; Maharana, S.; Lemaitre, R.; Pozniakovsky, A.; Drechsel, D.; et al. A Molecular Grammar Governing the Driving Forces for Phase Separation of Prion-like RNA Binding Proteins. *Cell* **2018**, *174*, 688–699.e16. [CrossRef]
19. Ying, Y.; Wang, X.J.; Vuong, C.K.; Lin, C.H.; Damianov, A.; Black, D.L. Splicing Activation by Rbfox Requires Self-Aggregation through Its Tyrosine-Rich Domain. *Cell* **2017**, *170*, 312–323.e10. [CrossRef]
20. Gueroussov, S.; Weatheritt, R.J.; O'Hanlon, D.; Lin, Z.Y.; Narula, A.; Gingras, A.C.; Blencowe, B.J. Regulatory Expansion in Mammals of Multivalent hnRNP Assemblies that Globally Control Alternative Splicing. *Cell* **2017**, *170*, 324–339.e23. [CrossRef]
21. Conicella, A.E.; Zerze, G.H.; Mittal, J.; Fawzi, N.L. ALS Mutations Disrupt Phase Separation Mediated by alpha-Helical Structure in the TDP-43 Low-Complexity C-Terminal Domain. *Structure* **2016**, *24*, 1537–1549. [CrossRef] [PubMed]
22. Burke, K.A.; Janke, A.M.; Rhine, C.L.; Fawzi, N.L. Residue-by-Residue View of In Vitro FUS Granules that Bind the C-Terminal Domain of RNA Polymerase II. *Mol. Cell* **2015**, *60*, 231–241. [CrossRef] [PubMed]
23. Li, H.R.; Chen, T.C.; Hsiao, C.L.; Shi, L.; Chou, C.Y.; Huang, J.R. The physical forces mediating self-association and phase-separation in the C-terminal domain of TDP-43. *Biochim. Biophys. Acta* **2018**, *1866*, 214–223. [CrossRef] [PubMed]
24. Ryan, V.H.; Dignon, G.L.; Zerze, G.H.; Chabata, C.V.; Silva, R.; Conicella, A.E.; Amaya, J.; Burke, K.A.; Mittal, J.; Fawzi, N.L. Mechanistic View of hnRNPA2 Low-Complexity Domain Structure, Interactions, and Phase Separation Altered by Mutation and Arginine Methylation. *Mol. Cell* **2018**, *69*, 465–479.e7. [CrossRef] [PubMed]
25. Fox, R.G.; Park, F.D.; Koechlein, C.S.; Kritzik, M.; Reya, T. Musashi signaling in stem cells and cancer. *Annu. Rev. Cell Dev. Biol.* **2015**, *31*, 249–267. [CrossRef] [PubMed]
26. Sengupta, U.; Montalbano, M.; McAllen, S.; Minuesa, G.; Kharas, M.; Kayed, R. Formation of Toxic Oligomeric Assemblies of RNA-binding Protein: Musashi in Alzheimer's disease. *Acta Neuropathol. Commun.* **2018**, *6*, 113. [CrossRef] [PubMed]
27. Montalbano, M.; McAllen, S.; Sengupta, U.; Puangmalai, N.; Bhatt, N.; Ellsworth, A.; Kayed, R. Tau oligomers mediate aggregation of RNA-binding proteins Musashi1 and Musashi2 inducing Lamin alteration. *Aging Cell* **2019**, *18*, e13035. [CrossRef] [PubMed]
28. Wang, I.F.; Wu, L.S.; Shen, C.K. TDP-43: An emerging new player in neurodegenerative diseases. *Trends Mol. Med.* **2008**, *14*, 479–485. [CrossRef]
29. Taylor, J.P.; Brown, R.H., Jr.; Cleveland, D.W. Decoding ALS: From genes to mechanism. *Nature* **2016**, *539*, 197–206. [CrossRef]
30. Chen, H.Y.; Lin, L.T.; Wang, M.L.; Tsai, K.L.; Huang, P.I.; Yang, Y.P.; Lee, Y.Y.; Chen, Y.W.; Lo, W.L.; Lan, Y.T.; et al. Musashi-1 promotes chemoresistant granule formation by PKR/eIF2alpha signalling cascade in refractory glioblastoma. *Biochim. Biophys. Acta Mol. Basis Dis.* **2018**, *1864*, 1850–1861. [CrossRef]
31. Chiou, G.Y.; Yang, T.W.; Huang, C.C.; Tang, C.Y.; Yen, J.Y.; Tsai, M.C.; Chen, H.Y.; Fadhilah, N.; Lin, C.C.; Jong, Y.J. Musashi-1 promotes a cancer stem cell lineage and chemoresistance in colorectal cancer cells. *Sci. Rep.* **2017**, *7*, 2172. [CrossRef]
32. Sigrist, C.J.; Cerutti, L.; De Castro, E.; Langendijk-Genevaux, P.S.; Bulliard, V.; Bairoch, A.; Hulo, N. PROSITE, a protein domain database for functional characterization and annotation. *Nucleic Acids Res.* **2010**, *38*, D161–D166. [CrossRef] [PubMed]
33. Iwaoka, R.; Nagata, T.; Tsuda, K.; Imai, T.; Okano, H.; Kobayashi, N.; Katahira, M. Structural Insight into the Recognition of r(UAG) by Musashi-1 RBD2, and Construction of a Model of Musashi-1 RBD1-2 Bound to the Minimum Target RNA. *Molecules* **2017**, *22*, 1207. [CrossRef] [PubMed]
34. Ohyama, T.; Nagata, T.; Tsuda, K.; Kobayashi, N.; Imai, T.; Okano, H.; Yamazaki, T.; Katahira, M. Structure of Musashi1 in a complex with target RNA: The role of aromatic stacking interactions. *Nucleic Acids Res.* **2012**, *40*, 3218–3231. [CrossRef]
35. Wootton, J.C. Non-globular domains in protein sequences: Automated segmentation using complexity measures. *Comput. Chem.* **1994**, *18*, 269–285. [CrossRef]
36. Prilusky, J.; Felder, C.E.; Zeev-Ben-Mordehai, T.; Rydberg, E.H.; Man, O.; Beckmann, J.S.; Silman, I.; Sussman, J.L. FoldIndex: A simple tool to predict whether a given protein sequence is intrinsically unfolded. *Bioinformatics* **2005**, *21*, 3435–3438. [CrossRef] [PubMed]

37. Radivojac, P.; Obradović, Z.; Brown, C.J.; Dunker, A.K. Prediction of boundaries between intrinsically ordered and disordered protein regions. *Pac. Symp. Biocomput.* **2003**, *8*, 216–227.
38. Kyte, J.; Doolittle, R.F. A simple method for displaying the hydropathic character of a protein. *J. Mol. Biol.* **1982**, *157*, 105–132. [CrossRef]
39. Lancaster, A.K.; Nutter-Upham, A.; Lindquist, S.; King, O.D. PLAAC: A web and command-line application to identify proteins with prion-like amino acid composition. *Bioinformatics* **2014**, *30*, 2501–2502. [CrossRef]
40. Walsh, I.; Seno, F.; Tosatto, S.C.; Trovato, A. PASTA 2.0: An improved server for protein aggregation prediction. *Nucleic Acids Res.* **2014**, *42*, W301–W307. [CrossRef]
41. Camilloni, C.; De Simone, A.; Vranken, W.F.; Vendruscolo, M. Determination of secondary structure populations in disordered states of proteins using nuclear magnetic resonance chemical shifts. *Biochemistry* **2012**, *51*, 2224–2231. [CrossRef] [PubMed]
42. Micsonai, A.; Wien, F.; Bulyáki, É.; Kun, J.; Moussong, É.; Lee, Y.H.; Goto, Y.; Réfrégiers, M.; Kardos, J. BeStSel: A web server for accurate protein secondary structure prediction and fold recognition from the circular dichroism spectra. *Nucleic Acids Res.* **2018**, *46*, W315–W322. [CrossRef] [PubMed]
43. Micsonai, A.; Wien, F.; Kernya, L.; Lee, Y.H.; Goto, Y.; Réfrégiers, M.; Kardos, J. Accurate secondary structure prediction and fold recognition for circular dichroism spectroscopy. *Proc. Natl. Acad. Sci. USA* **2015**, *112*, E3095–E3103. [CrossRef]
44. Xiang, S.; Kato, M.; Wu, L.C.; Lin, Y.; Ding, M.; Zhang, Y.; Yu, Y.; McKnight, S.L. The LC Domain of hnRNPA2 Adopts Similar Conformations in Hydrogel Polymers, Liquid-like Droplets, and Nuclei. *Cell* **2015**, *163*, 829–839. [CrossRef] [PubMed]
45. Nott, T.J.; Petsalaki, E.; Farber, P.; Jervis, D.; Fussner, E.; Plochowietz, A.; Craggs, T.D.; Bazett-Jones, D.P.; Pawson, T.; Forman-Kay, J.D.; et al. Phase transition of a disordered nuage protein generates environmentally responsive membraneless organelles. *Mol. Cell* **2015**, *57*, 936–947. [CrossRef]
46. Fang, X.; Wang, L.; Ishikawa, R.; Li, Y.; Fiedler, M.; Liu, F.; Calder, G.; Rowan, B.; Weigel, D.; Li, P.; et al. Arabidopsis FLL2 promotes liquid-liquid phase separation of polyadenylation complexes. *Nature* **2019**, *569*, 265–269. [CrossRef]
47. Brown, L.Y.; Brown, S.A. Alanine tracts: The expanding story of human illness and trinucleotide repeats. *Trends Genet.* **2004**, *20*, 51–58. [CrossRef]
48. Li, L.; Ng, N.K.; Koon, A.C.; Chan, H.Y. Expanded polyalanine tracts function as nuclear export signals and promote protein mislocalization via eEF1A1 factor. *J. Biol. Chem.* **2017**, *292*, 5784–5800. [CrossRef]
49. Polling, S.; Ormsby, A.R.; Wood, R.J.; Lee, K.; Shoubridge, C.; Hughes, J.N.; Thomas, P.Q.; Griffin, M.D.; Hill, A.F.; Bowden, Q.; et al. Polyalanine expansions drive a shift into alpha-helical clusters without amyloid-fibril formation. *Nat. Struct. Mol. Biol.* **2015**, *22*, 1008–1015. [CrossRef]
50. Itakura, A.K.; Futia, R.A.; Jarosz, D.F. It Pays To Be in Phase. *Biochemistry* **2018**, *57*, 2520–2529. [CrossRef]
51. Dominguez, D.; Freese, P.; Alexis, M.S.; Su, A.; Hochman, M.; Palden, T.; Bazile, C.; Lambert, N.J.; Van Nostrand, E.L.; Pratt, G.A.; et al. Sequence, Structure, and Context Preferences of Human RNA Binding Proteins. *Mol. Cell* **2018**, *70*, 854–867.e9. [CrossRef] [PubMed]
52. Wilkins, M.R.; Gasteiger, E.; Bairoch, A.; Sanchez, J.C.; Williams, K.L.; Appel, R.D.; Hochstrasser, D.F. Protein identification and analysis tools in the ExPASy server. *Methods Mol. Biol.* **1999**, *112*, 531–552.
53. UniProt Consortium. UniProt: A worldwide hub of protein knowledge. *Nucleic Acids Res.* **2019**, *47*, D506–D515. [CrossRef]
54. Yoshimura, Y.; Kulminskaya, N.V.; Mulder, F.A. Easy and unambiguous sequential assignments of intrinsically disordered proteins by correlating the backbone 15N or 13C′ chemical shifts of multiple contiguous residues in highly resolved 3D spectra. *J. Biomol. NMR* **2015**, *61*, 109–121. [CrossRef] [PubMed]
55. Kjaergaard, M.; Brander, S.; Poulsen, F.M. Random coil chemical shift for intrinsically disordered proteins: Effects of temperature and pH. *J. Biomol. NMR* **2011**, *49*, 139–149. [CrossRef] [PubMed]
56. Piotto, M.; Saudek, V.; Sklenar, V. Gradient-tailored excitation for single-quantum NMR spectroscopy of aqueous solutions. *J. Biomol. NMR* **1992**, *2*, 661–665. [CrossRef]
57. Liu, M.; Mao, X.A.; Ye, C.; Huang, H.; Nicholson, J.K.; Lindon, J.C. Improved WATERGATE Pulse Sequences for Solvent Suppression in NMR Spectroscopy. *J. Magn. Reson.* **1998**, *132*, 125–129. [CrossRef]
58. Kay, L.E.; Torchia, D.A.; Bax, A. Backbone dynamics of proteins as studied by 15N inverse detected heteronuclear NMR spectroscopy: Application to staphylococcal nuclease. *Biochemistry* **1989**, *28*, 8972–8979. [CrossRef]

59. Greenfield, N.J. Using circular dichroism spectra to estimate protein secondary structure. *Nat. Protoc.* **2006**, *1*, 2876–2890. [CrossRef]
60. Dubochet, J. On the Development of Electron Cryo-Microscopy (Nobel Lecture). *Angew. Chem. Int. Ed.* **2018**, *57*, 10842–10846. [CrossRef]
61. Henderson, R. From Electron Crystallography to Single Particle CryoEM (Nobel Lecture). *Angew. Chem. Int. Ed.* **2018**, *57*, 10804–10825. [CrossRef] [PubMed]
62. Frank, J. Single-Particle Reconstruction of Biological Molecules-Story in a Sample (Nobel Lecture). *Angew. Chem. Int. Ed.* **2018**, *57*, 10826–10841. [CrossRef] [PubMed]
63. Fernandez-Leiro, R.; Scheres, S.H. Unravelling biological macromolecules with cryo-electron microscopy. *Nature* **2016**, *537*, 339–346. [CrossRef] [PubMed]
64. Callaway, E. The revolution will not be crystallized: A new method sweeps through structural biology. *Nature* **2015**, *525*, 172–174. [CrossRef] [PubMed]
65. Dyson, H.J.; Wright, P.E. Perspective: The essential role of NMR in the discovery and characterization of intrinsically disordered proteins. *J. Biomol. NMR* **2019**, *73*, 651–659. [CrossRef] [PubMed]
66. Kawahara, H.; Imai, T.; Imataka, H.; Tsujimoto, M.; Matsumoto, K.; Okano, H. Neural RNA-binding protein Musashi1 inhibits translation initiation by competing with eIF4G for PABP. *J. Cell Biol.* **2008**, *181*, 639–653. [CrossRef]
67. Cragle, C.; MacNicol, A.M. Musashi protein-directed translational activation of target mRNAs is mediated by the poly(A) polymerase, germ line development defective-2. *J. Biol. Chem.* **2014**, *289*, 14239–14251. [CrossRef]

Supporting Information

Musashi-1: an example of how polyalanine tracts contribute to self-association in the intrinsically disordered regions of RNA-binding proteins

Tsai-Chen Chen and Jie-rong Huang

Institute of Biochemistry and Molecular Biology and Institute of Biomedical Informatics,

National Yang-Ming University, No. 155 Section 2 Li-nong Street, Taipei, Taiwan

Assignment strategy

We followed a denaturation-then-titration strategy – assigning the protein under harsh conditions and then titrating back to physiological conditions – because Musashi-1's IDR has a strong tendency to aggregate. We also used (H)N(COCO)NH and (HN)CO(CO)NH pulse sequences to help complete the sequential assignment, using long-range (*i*, *i*+2) connections between backbone nitrogen and carbonyl-carbon atoms to overcome disruptions due to the 20 prolines (which make up about 12 % in the primary sequence).

We first prepared the 0.7 mM ^{15}N/^{13}C-labeled sample in 10 mM glycine buffer with 8 M urea at pH 2.5, conditions under which the NMR peaks are well-dispersed (Figure A1). The assignment was facilitated by (H)N(COCO)NH and (HN)CO(CO)NH data. ^{15}N-labeled samples of four different constructs were used to distinguish assignments that remained ambiguous (Figure A2) under the same buffer condition. ^{15}N-labeled sample (~70 μM) in 10 mM phosphate buffer at pH 5.5 was titrated to different pHs till pH=2.5 using phosphoric acid (Figure A3). ^{15}N-labeled samples (~70 μM) in 20 mM MES buffer at pH 5.5 with urea concentrations ranging from 0 to 8 M are shown in Figure A4. Finally, all the triple resonance assignment experiments were applied to the ^{15}N/^{13}C-labeled sample (~130 μM) in 20 mM MES at pH 5.5 to confirm the assignment.

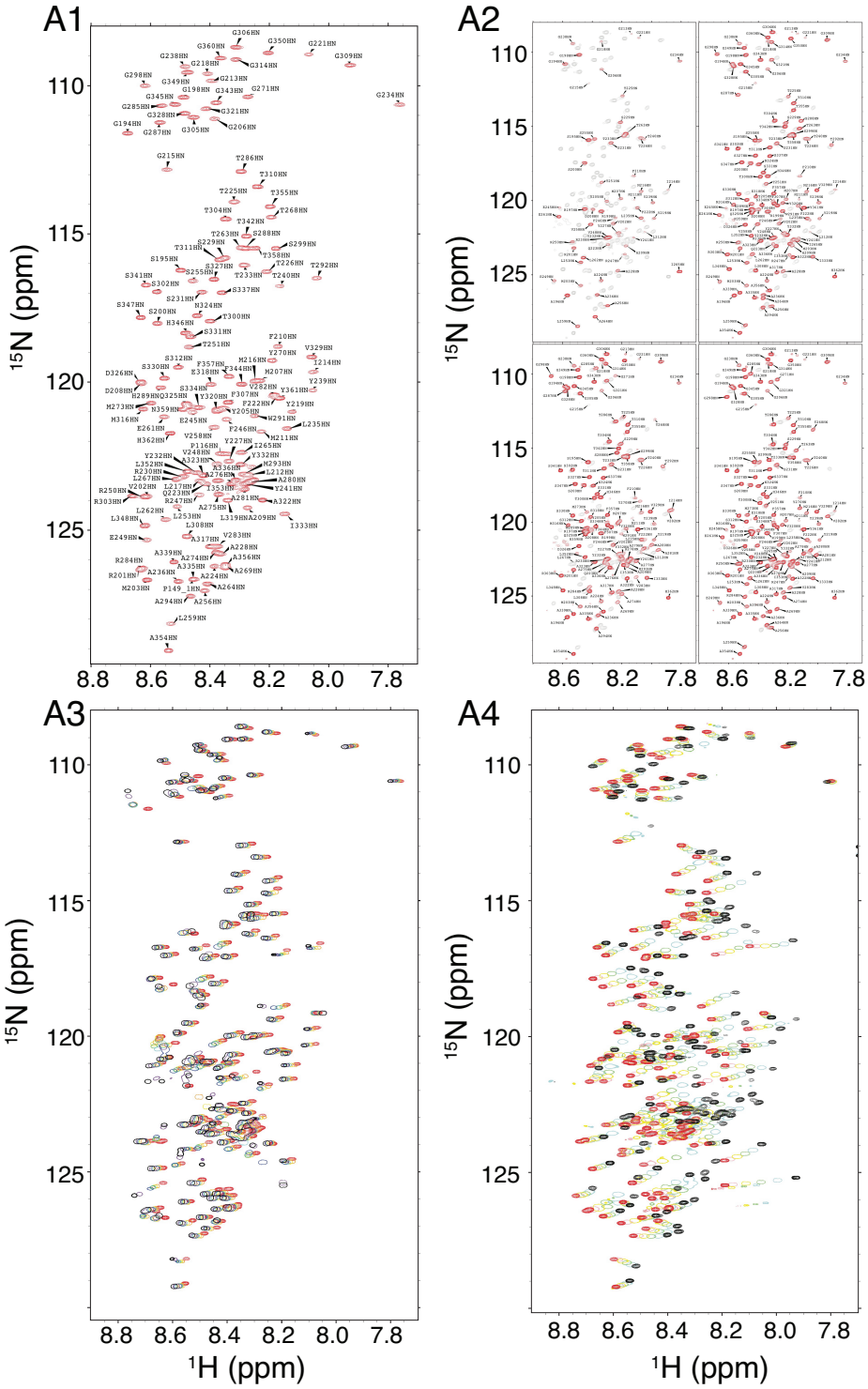

A1. Chemical shift Assignment in the presence 8 M urea at pH 2.5. **A2**. HSQC spectra of four different truncated contracts (red, also see Table S1) overlaid with the wild-type (grey). **A3.** Titration of pH from 2.5 (red) to 5.5 (black) in the presence of 8 M urea. **A4**. Titration of urea from 8 M (red) to zero (black) at pH 5.5.

Supporting Figures:

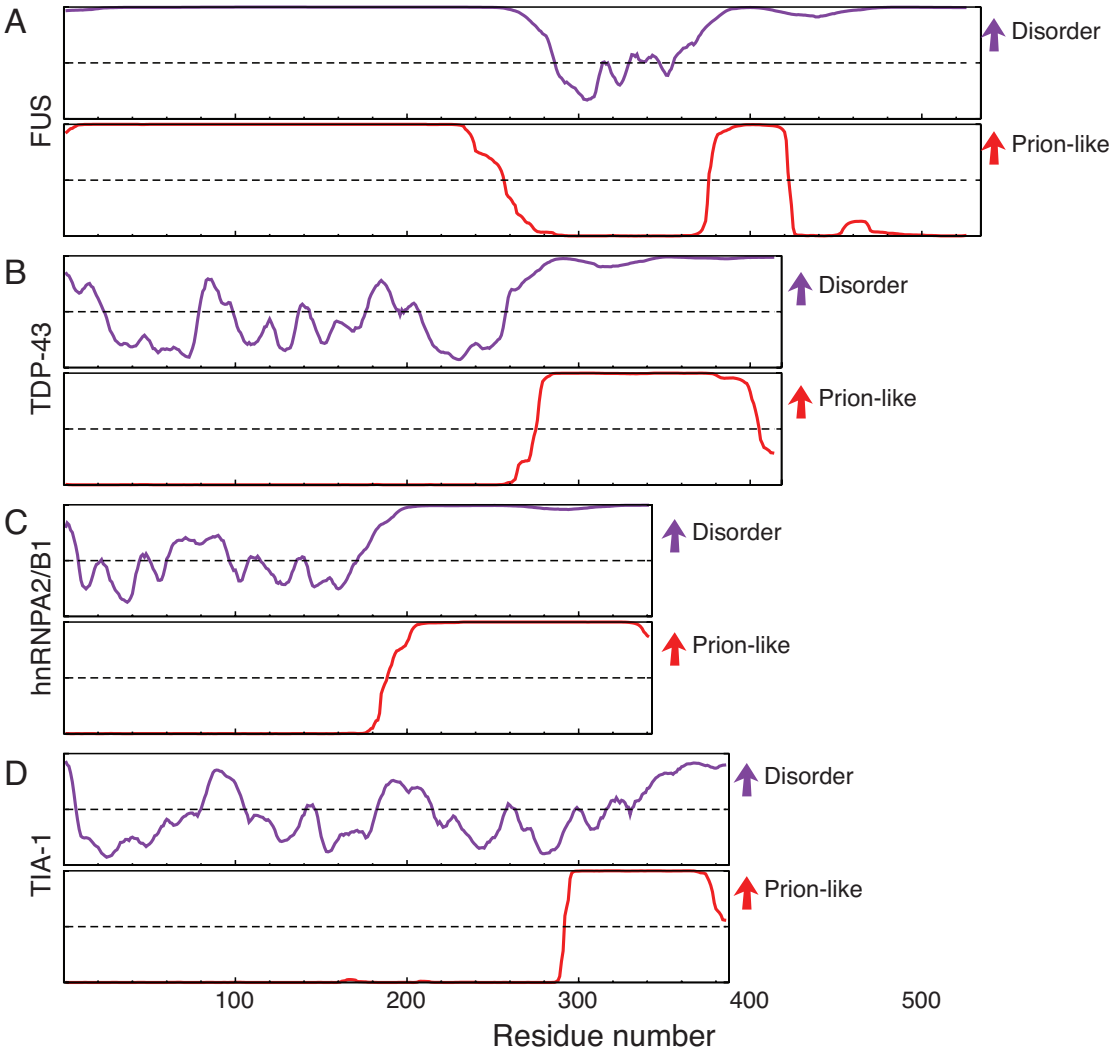

Figure S1. RNA binding proteins involved in neurodegenerative diseases have intrinsically disordered regions (purple) with prion-likeness (red). (**A**) FUS, (**B**) TDP-43, (**C**) hnRNPA2/B1, (**D**) TIA-1.

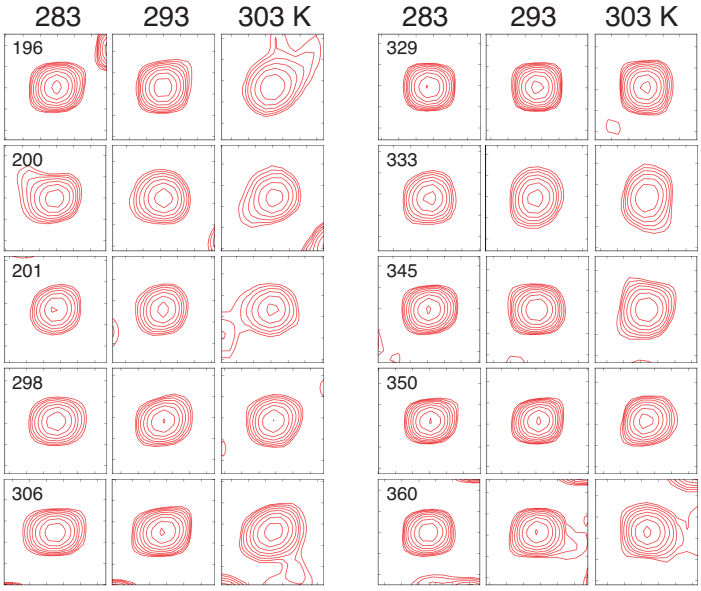

Figure S2. In contrast with Figure 3B: examples of peaks in the HSQC spectra that show little line-broadening or distortion at any of the three temperatures.

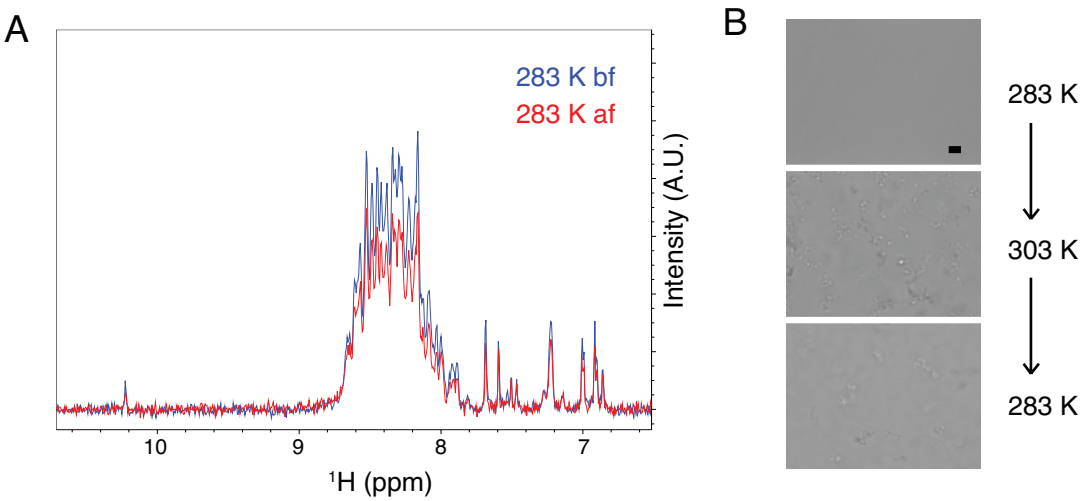

Figure S3. Irreversibility of Musashi-1 oligomerization. (**A**) NMR spectra of Musashi-1 samples before (blue) and after heating to 303 K (red). (**B**) Sequence of micrographs of a (fresh) Musashi-1 sample at 283 K, 303 K and then 283 K once again. Scale bar: 5 µm.

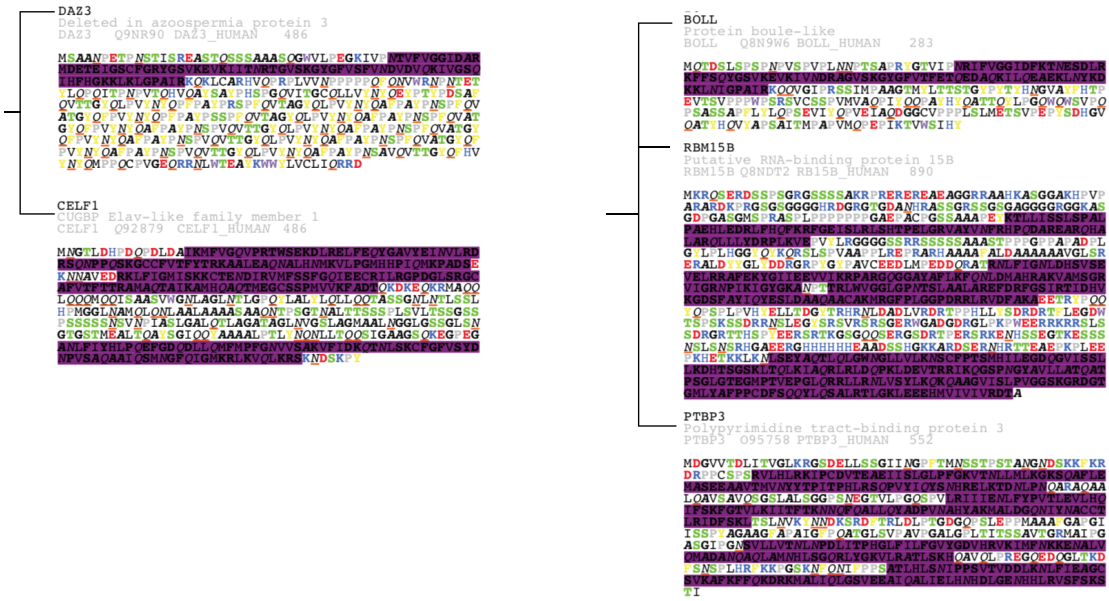

Figure S4. Examples of RBPs that bind to similar RNA motifs but whose IDRs have different properties. The amino acids are coloured according to their physical properties (Positive charge: blue; negative charge: red; F/Y: yellow; W: purple; S/T (potential phosphorylation site for the addition of negative charges): green; P: grey; A: italic-bold black; Q/N: red underlined italic)

Supporting Information: Tables

Table S1. Primers used in this study.

Constructs	Primers
His-MSI-1C	Fw-5'-AAAAAACATATGCATCATCATCATCATCATGGCAGCGCGCGC-3'
a.a. 194-362	(*NdeI*)
	Rv-5'-AAAAACTCGAGTCAGTGGTACCCA-3' (*XhoI*)
His-MSI-1CΔS1	Fw-5'-CCCGAATTCCCTCTCACTGCCTACGGACCA-3'
247-265 deleted	Rv-5'-AGTGAGAGGGAATTCGGGGAACTGGTAGGT-3'
His-MSI-1CΔS2	Fw-5'-GGGACAGGTTCGACTCCCAGCCGCAC-3'
287-297 deleted	Rv-5'-CGAACCTGTCCCTCGAACCACAGCCG-3'
His-MSI-1CΔA2	Fw-5'-ACAGCCATTGGCTCTCACCCCTGGACGATG-3'
266-286 deleted	Rv-5'-GTGAGAGCCAATGGCTGTAAGCTCGGGGAG-3'
His-MSI-1Cnt	Fw-5'-CATTTAATAAACTGCCTACGGACCAATGGC-3'
a.a. 194-265	Rv-5'-AGTTTATTAAATGGCTGTAAGCTCGGGGAG-3'

Table S2. Number of human proteins with different lengths of alanine repeats related to RNA functions.

N-alanine repeats	Number of *N*-alanine-repeats with an RNA-related GO	Number of *N*-alanine-repeats with an "RNA-binding" GO	Total number of proteins containing *N*-alanine repeats
5	319	97	687
6	221	57	411
7	164	41	262
8	115	24	178
9	91	17	132
10	69	14	95
11	49	5	71
12	39	5	55
13	32	4	45
14	23	2	32
15	16	0	23
16	11	0	16
17	3	0	6
18	2	0	4
19	1	0	3
20	1	0	2
21	0	0	1

GO, gene annotation.

Table S3. List of RBPs in Dominguez et al.'s study with polyalanine tracts.

Gene name	Protein name	Entry	*N*-alanine
RBM47	RNA-binding protein 47	A0AV96	14, 6
RBM24	RNA-binding protein 24	Q9BX46	11, 13
RBM4	RNA-binding protein 4	Q9BWF3	10, 5
RBM23	Probable RNA-binding protein 23	Q86U06	9
RBFOX2	RNA binding protein fox-1 homolog 2	O43251	8
MSI1	RNA-binding protein Musashi homolog 1	O43347	8
MBNL1	Muscleblind-like protein 1	MBNL1	7
PUM1	Pumilio homolog 1	Q14671	7, 5
RBM15B	Putative RNA-binding protein 15B	Q8NDT2	6
RBM4B	RNA-binding protein 4B	Q9BQ04	6, 5
RBFOX3	RNA binding protein fox-1 homolog 3	A6NFN3	6
HNRNPDL	Heterogeneous nuclear ribonucleoprotein D-like	O14979	6
KHSRP	Far upstream element-binding protein 2	Q92945	6
SF1	Splicing factor 1	Q15637	5
A1CF	APOBEC1 complementation factor	Q9NQ94	5
HNRNPD	Heterogeneous nuclear ribonucleoprotein D0	Q14103	5, 5
NOVA1	RNA-binding protein Nova-1	P51513	5, 5, 5
PUF60	Poly(U)-binding-splicing factor	Q9UHX1	5, 5

Appendix

Chemical shift assignment

RES		CA	CB	CO	N	HN
194	G	45.006	0.0	173.819	110.654	8.479
195	S	58.085	64.004	174.313	115.761	8.318
196	A	52.533	19.042	177.669	126.252	8.457
197	R	56.145	30.696	176.789	120.460	8.338
198	G	45.049	0.0	173.838	110.044	8.376
199	R	55.938	30.799	176.342	120.578	8.235
200	S	58.231	63.874	174.217	117.318	8.340
201	R	56.119	30.758	175.833	123.025	8.413
202	V	62.279	32.520	175.723	121.367	8.149
203	M	52.736	32.374	174.087	125.521	8.364
204	P	63.067	31.881	176.092	0.0	0.0
205	Y	58.018	38.570	176.271	119.824	8.181
206	G	45.149	0.0	174.316	110.905	8.230
207	M	55.819	32.523	176.096	119.738	8.108
208	D	54.819	40.898	176.431	120.403	8.291
209	A	53.525	18.616	178.275	122.840	8.062
210	F	0.0	39.047	176.473	118.164	8.014
211	M	0.0	0.0	175.085	119.721	8.017
212	L	55.217	0.0	177.810	121.875	7.945
213	G	45.380	0.0	174.205	108.570	8.031
214	I	61.645	0.0	176.803	119.044	7.773
215	G	45.422	0.0	174.184	111.882	8.310
216	M	55.325	32.852	175.397	119.205	7.969
217	L	0.0	0.0	177.508	0.0	0.0
218	G	44.840	0.0	173.258	109.036	8.219
219	Y	55.881	38.008	174.144	121.015	7.878
220	P	63.774	31.675	177.166	0.0 0.0	
221	G	45.160	0.0	173.895	108.794	7.975
222	F	58.275	39.489	175.524	120.327	7.999
223	Q	55.425	29.498	174.981	122.706	8.189
224	A	52.758	19.150	177.961	125.211	8.231
225	T	62.023	69.716	174.723	112.755	8.083
226	T	61.908	69.725	174.281	115.626	7.964
227	Y	58.229	38.581	175.716	122.010	8.114
228	A	52.635	19.112	177.545	124.590	8.119
229	S	58.551	63.656	174.636	114.563	8.104
230	R	56.164	30.557	175.981	122.332	8.202
231	S	58.124	63.766	173.963	115.968	8.165
232	Y	57.909	38.758	175.900	122.287	8.189
233	T	61.763	69.693	174.695	115.400	8.077
234	G	45.090	0.0	173.450	110.435	7.715
235	L	54.534	42.450	176.726	121.039	7.957
236	A	50.434	17.997	175.186	126.176	8.251
237	P	63.439	31.831	177.419	0.0 0.0	
238	G	45.125	0.0	173.837	109.209	8.414
239	Y	58.130	39.073	175.663	119.925	7.881
240	T	61.461	70.096	173.549	115.668	7.943
241	Y	58.059	0.0	0.0	122.313	8.010
242	Q	0.0	0.0	0.0	0.0	0.0
243	F	0.0	0.0	0.0	0.0	0.0
244	P	63.337	31.864	176.530	0.0	0.0
245	E	56.624	30.040	175.992	120.300	8.501
246	F	57.468	39.492	175.093	121.040	8.138

247	R	55.595	31.045	175.389	123.456	8.083
248	V	62.234	32.604	175.926	122.243	8.175
249	E	56.182	30.211	176.039	125.257	8.544
250	R	55.762	30.730	176.007	122.624	8.423
251	T	59.916	69.638	172.539	118.662	8.232
252	P	62.887	32.054	176.537	0.0 0.0	
253	L	53.009	41.444	175.437	123.993	8.357
254	P	63.119	31.897	176.731	0.0 0.0	
255	S	58.032	63.747	173.660	115.759	8.277
256	A	50.432	18.199	175.186	126.933	8.196
257	P	62.838	31.954	176.458	0.0 0.0	
258	V	62.082	32.608	175.976	121.356	8.286
259	L	52.708	41.435	175.034	128.212	8.372
260	P	62.988	31.919	176.730	0.0 0.0	
261	E	56.429	30.024	176.532	120.806	8.530
262	L	55.173	42.042	177.387	123.570	8.336
263	T	61.788	69.707	173.860	114.897	8.028
264	A	52.106	19.182	177.160	126.731	8.224
265	I	58.669	38.500	174.518	122.479	8.140
266	P	62.927	32.077	176.777	0.0 0.0	
267	L	55.570	42.019	177.792	122.591	8.401
268	T	61.694	69.707	174.081	113.468	7.912
269	A	52.348	19.192	176.955	125.635	8.154
270	Y	57.803	38.996	176.040	118.801	7.999
271	G	45.018	0.0	172.363	110.154	8.155
272	P	63.967	31.912	178.068	0.0 0.0	
273	M	56.370	32.202	177.006	119.278	8.354
274	A	53.373	18.552	178.697	124.858	8.107
275	A	53.537	18.455	178.961	122.700	8.222
276	A	53.474	18.382	178.963	122.463	8.114
277	A	53.401	18.442	178.887	122.543	8.015
278	A	53.383	18.419	178.725	122.360	8.050
279	A	53.244	18.469	178.510	121.844	7.971
280	A	52.904	18.647	178.038	121.585	7.921
281	A	52.874	18.723	178.213	121.877	7.881
282	V	63.120	32.328	176.652	119.202	7.798
283	V	62.902	32.287	176.376	123.871	8.034
284	R	56.380	30.725	176.786	124.522	8.336
285	G	45.162	0.0	174.357	109.550	8.289
286	T	61.911	69.797	175.267	113.055	8.139
287	G	45.175	0.0	173.942	110.983	8.473
288	S	58.145	63.687	173.831	115.145	8.124
289	H	53.103	28.591	172.430	120.143	8.339
290	P	63.457	31.825	176.508	0.0 0.0	
291	W	57.379	29.152	176.153	120.363	8.065
292	T	61.536	69.916	173.565	116.164	7.816
293	M	55.077	32.947	175.162	122.479	8.052
294	A	50.331	17.906	174.694	127.062	8.262
295	P	0.0	0.0	0.0	0.0	0.0
296	P	0.0	0.0	0.0	0.0	0.0
297	P	63.344	31.832	177.549	0.0	0.0
298	G	45.123	0.0	174.181	109.892	8.557
299	S	58.371	63.988	174.183	115.337	8.063
300	T	59.827	69.718	172.715	118.193	8.272
301	P	63.248	32.049	176.811	0.0	0.0
302	S	58.229	63.715	174.745	116.295	8.419
303	R	56.137	30.696	176.478	123.419	8.492
304	T	61.802	69.675	175.013	114.431	8.177

305	G	45.262	0.0	174.355	111.130	8.370
306	G	44.910	0.0	173.692	108.475	8.195
307	F	57.823	39.492	175.828	120.161	8.159
308	L	55.006	42.236	177.368	124.532	8.304
309	G	45.214	0.0	174.007	109.020	7.834
310	T	61.595	69.848	174.687	113.250	8.049
311	T	61.650	69.818	174.168	116.196	8.209
312	S	56.299	63.302	172.574	119.742	8.360
313	P	63.349	32.097	176.956	0.0	0.0
314	G	44.454	0.0	0.0	109.122	8.196
315	P	63.309	31.950	177.362	0.0	0.0
316	M	55.527	32.455	176.152	120.063	8.451
317	A	52.879	19.105	177.875	124.642	8.160
318	E	56.579	29.888	176.381	119.496	8.302
319	L	55.254	42.245	177.148	0.0	0.0
320	Y	57.902	38.472	176.398	119.965	8.116
321	G	45.198	0.0	173.763	110.309	8.198
322	A	52.469	19.234	177.591	123.642	8.054
323	A	52.509	18.984	177.533	122.508	8.266
324	N	53.243	38.671	175.242	117.368	8.286
325	Q	55.951	29.294	175.667	120.497	8.327
326	D	54.354	41.076	176.365	121.438	8.377
327	S	58.771	63.684	175.147	116.771	8.307
328	G	45.320	0.0	174.173	110.761	8.455
329	V	62.319	32.570	176.374	119.095	7.894
330	S	58.393	63.703	174.534	119.359	8.414
331	S	58.389	63.703	173.913	117.897	8.250
332	Y	58.037	38.582	175.403	122.106	8.094
333	I	60.730	38.639	175.723	123.516	7.918
334	S	58.120	63.793	174.243	120.076	8.260
335	A	52.388	19.146	177.162	126.340	8.307
336	A	52.162	19.185	177.469	122.880	8.166
337	S	56.329	63.159	172.284	116.767	8.204
338	P	62.853	31.953	176.220	0.0	0.0
339	A	50.384	17.829	175.527	125.991	8.404
340	P	62.978	31.979	177.010	0.0	0.0
341	S	58.285	63.625	174.890	116.281	8.492
342	T	61.728	69.741	174.936	114.812	8.105
343	G	45.021	0.0	173.769	110.337	8.273
344	F	57.969	39.410	176.432	120.022	8.179
345	G	45.182	0.0	173.803	110.617	8.407
346	H	55.094	29.181	174.395	118.078	8.239
347	S	58.252	63.726	174.510	117.226	8.403
348	L	55.287	42.105	177.763	124.445	8.479
349	G	45.012	0.0	174.081	109.553	8.382
350	G	44.382	0.0	0.0	108.896	8.069
351	P	62.929	32.104	176.764	0.0	0.0
352	L	55.155	41.983	177.175	122.192	8.332
353	I	60.526	38.452	175.715	122.607	8.060
354	A	52.485	19.180	177.664	128.692	8.407
355	T	61.667	69.833	174.109	113.656	8.044
356	A	52.435	19.073	177.283	125.854	8.206
357	F	57.620	39.310	176.119	119.311	8.181
358	T	61.707	69.716	174.084	115.420	8.049
359	N	53.328	38.642	175.381	120.646	8.335
360	G	45.079	0.0	173.468	108.830	8.225
361	Y	57.961	38.555	174.837	120.314	7.983
362	H	56.718	29.873	178.140	124.925	7.776

Gene ontology annotations related to RNA

GO:0000049; F:tRNA binding; TAS:BHF-UCL.
GO:0000120; C:RNA polymerase I transcription factor complex; TAS:ProtInc.
GO:0000122; P:negative regulation of transcription by RNA polymerase II; TAS:UniProtKB.
GO:0000154; P:rRNA modification; TAS:Reactome.
GO:0000179; F:rRNA (adenine-N6,N6-)-dimethyltransferase activity; IMP:UniProtKB.
GO:0000184; P:nuclear-transcribed mRNA catabolic process, nonsense-mediated decay; TAS:UniProtKB.
GO:0000213; F:tRNA-intron endonuclease activity; IBA:GO_Central.
GO:0000214; C:tRNA-intron endonuclease complex; IEA:InterPro.
GO:0000215; F:tRNA 2'-phosphotransferase activity; TAS:UniProtKB.
GO:0000288; P:nuclear-transcribed mRNA catabolic process, deadenylation-dependent decay; TAS:UniProtKB.
GO:0000289; P:nuclear-transcribed mRNA poly(A) tail shortening; TAS:Reactome.
GO:0000290; P:deadenylation-dependent decapping of nuclear-transcribed mRNA; IEA:Ensembl.
GO:0000291; P:nuclear-transcribed mRNA catabolic process, exonucleolytic; IMP:UniProtKB.
GO:0000294; P:nuclear-transcribed mRNA catabolic process, endonucleolytic cleavage-dependent decay; ISS:UniProtKB.
GO:0000339; F:RNA cap binding; TAS:UniProtKB.
GO:0000340; F:RNA 7-methylguanosine cap binding; IMP:UniProtKB.
GO:0000375; P:RNA splicing, via transesterification reactions; TAS:UniProtKB.
GO:0000379; P:tRNA-type intron splice site recognition and cleavage; IBA:GO_Central.
GO:0000380; P:alternative mRNA splicing, via spliceosome; ISS:UniProtKB.
GO:0000381; P:regulation of alternative mRNA splicing, via spliceosome; ISS:UniProtKB.
GO:0000389; P:mRNA 3'-splice site recognition; TAS:HGNC-UCL.
GO:0000395; P:mRNA 5'-splice site recognition; IDA:UniProtKB.
GO:0000398; P:mRNA splicing, via spliceosome; TAS:UniProtKB.
GO:0000430; P:regulation of transcription from RNA polymerase II promoter by glucose; IC:BHF-UCL.
GO:0000432; P:positive regulation of transcription from RNA polymerase II promoter by glucose; ISS:BHF-UCL.
GO:0000435; P:positive regulation of transcription from RNA polymerase II promoter by galactose; IDA:UniProtKB.
GO:0000447; P:endonucleolytic cleavage in ITS1 to separate SSU-rRNA from 5.8S rRNA and LSU-rRNA from tricistronic rRNA transcript (SSU-rRNA, 5.8S rRNA, LSU-rRNA); ISS:UniProtKB.
GO:0000448; P:cleavage in ITS2 between 5.8S rRNA and LSU-rRNA of tricistronic rRNA transcript (SSU-rRNA, 5.8S rRNA, LSU-rRNA); IEA:Ensembl.
GO:0000451; P:rRNA 2'-O-methylation; TAS:Reactome.
GO:0000453; P:enzyme-directed rRNA 2'-O-methylation; IEA:UniProtKB-UniRule.
GO:0000454; P:snoRNA guided rRNA pseudouridine synthesis; ISS:BHF-UCL.
GO:0000455; P:enzyme-directed rRNA pseudouridine synthesis; IMP:UniProtKB.
GO:0000460; P:maturation of 5.8S rRNA; IMP:UniProtKB.
GO:0000461; P:endonucleolytic cleavage to generate mature 3'-end of SSU-rRNA from (SSU-rRNA, 5.8S rRNA, LSU-rRNA); IBA:GO_Central.
GO:0000462; P:maturation of SSU-rRNA from tricistronic rRNA transcript (SSU-rRNA, 5.8S rRNA, LSU-rRNA); ISS:UniProtKB.
GO:0000463; P:maturation of LSU-rRNA from tricistronic rRNA transcript (SSU-rRNA, 5.8S rRNA, LSU-rRNA); IMP:UniProtKB.
GO:0000466; P:maturation of 5.8S rRNA from tricistronic rRNA transcript (SSU-rRNA, 5.8S rRNA, LSU-rRNA); IMP:UniProtKB.
GO:0000467; P:exonucleolytic trimming to generate mature 3'-end of 5.8S rRNA from tricistronic rRNA transcript (SSU-rRNA, 5.8S rRNA, LSU-rRNA); IBA:GO_Central.
GO:0000469; P:cleavage involved in rRNA processing; IEA:InterPro.
GO:0000470; P:maturation of LSU-rRNA; IBA:GO_Central.
GO:0000472; P:endonucleolytic cleavage to generate mature 5'-end of SSU-rRNA from (SSU-rRNA, 5.8S rRNA, LSU-rRNA); ISS:UniProtKB.
GO:0000480; P:endonucleolytic cleavage in 5'-ETS of tricistronic rRNA transcript (SSU-rRNA, 5.8S rRNA, LSU-rRNA); ISS:UniProtKB.
GO:0000481; P:maturation of 5S rRNA; IBA:GO_Central.
GO:0000494; P:box C/D snoRNA 3'-end processing; IBA:GO_Central.
GO:0000495; P:box H/ACA snoRNA 3'-end processing; IDA:UniProtKB.
GO:0000900; F:translation repressor activity, mRNA regulatory element binding; NAS:UniProtKB.
GO:0000956; P:nuclear-transcribed mRNA catabolic process; IMP:UniProtKB.
GO:0000957; P:mitochondrial RNA catabolic process; IDA:UniProtKB.
GO:0000958; P:mitochondrial mRNA catabolic process; IMP:UniProtKB.
GO:0000959; P:mitochondrial RNA metabolic process; IMP:UniProtKB.
GO:0000961; P:negative regulation of mitochondrial RNA catabolic process; IEA:Ensembl.
GO:0000962; P:positive regulation of mitochondrial RNA catabolic process; IDA:UniProtKB.
GO:0000963; P:mitochondrial RNA processing; IMP:UniProtKB.
GO:0000964; P:mitochondrial RNA 5'-end processing; IMP:UniProtKB.
GO:0000965; P:mitochondrial RNA 3'-end processing; IMP:UniProtKB.
GO:0000966; P:RNA 5'-end processing; ISS:UniProtKB.
GO:0000971; P:tRNA exon ligation utilizing 2',3' cyclic phosphate of 5'-exon as source of linkage phosphate; IBA:GO_Central.
GO:0000972; P:transcription-dependent tethering of RNA polymerase II gene DNA at nuclear periphery; ISS:BHF-UCL.

GO:0000973; P:posttranscriptional tethering of RNA polymerase II gene DNA at nuclear periphery; IBA:GO_Central.
GO:0000977; F:RNA polymerase II regulatory region sequence-specific DNA binding; ISS:UniProtKB.
GO:0000978; F:RNA polymerase II cis-regulatory region sequence-specific DNA binding; ISS:UniProtKB.
GO:0000979; F:RNA polymerase II core promoter sequence-specific DNA binding; ISS:UniProtKB.
GO:0000981; F:DNA-binding transcription factor activity, RNA polymerase II-specific; TAS:ProtInc.
GO:0000993; F:RNA polymerase II complex binding; ISS:UniProtKB.
GO:0000994; F:RNA polymerase III core binding; IBA:GO_Central.
GO:0000995; F:RNA polymerase III general transcription initiation factor activity; IMP:UniProtKB.
GO:0001002; F:RNA polymerase III type 1 promoter sequence-specific DNA binding; IBA:GO_Central.
GO:0001003; F:RNA polymerase III type 2 promoter sequence-specific DNA binding; IBA:GO_Central.
GO:0001004; F:RNA polymerase III transcription regulator recruiting activity; IEA:InterPro.
GO:0001006; F:RNA polymerase III type 3 promoter sequence-specific DNA binding; IBA:GO_Central.
GO:0001010; F:RNA polymerase II sequence-specific DNA-binding transcription factor recruiting activity; ISS:BHF-UCL.
GO:0001012; F:RNA polymerase II regulatory region DNA binding; IEA:Ensembl.
GO:0001013; F:RNA polymerase I regulatory region DNA binding; IDA:UniProtKB.
GO:0001016; F:RNA polymerase III regulatory region DNA binding; IDA:UniProtKB.
GO:0001030; F:RNA polymerase III type 1 promoter DNA binding; IDA:UniProtKB.
GO:0001031; F:RNA polymerase III type 2 promoter DNA binding; IDA:UniProtKB.
GO:0001032; F:RNA polymerase III type 3 promoter DNA binding; IDA:UniProtKB.
GO:0001042; F:RNA polymerase I core binding; ISS:UniProtKB.
GO:0001054; F:RNA polymerase I activity; IMP:ParkinsonsUK-UCL.
GO:0001055; F:RNA polymerase II activity; IEA:InterPro.
GO:0001069; F:regulatory region RNA binding; IEA:Ensembl.
GO:0001080; P:nitrogen catabolite activation of transcription from RNA polymerase II promoter; IC:BHF-UCL.
GO:0001085; F:RNA polymerase II transcription factor binding; ISS:BHF-UCL.
GO:0001091; F:RNA polymerase II general transcription initiation factor binding; IPI:ParkinsonsUK-UCL.
GO:0001099; F:basal RNA polymerase II transcription machinery binding; ISS:UniProtKB.
GO:0001102; F:RNA polymerase II activating transcription factor binding; TAS:BHF-UCL.
GO:0001103; F:RNA polymerase II repressing transcription factor binding; ISS:BHF-UCL.
GO:0001113; P:transcriptional open complex formation at RNA polymerase II promoter; IBA:GO_Central.
GO:0001135; F:RNA polymerase II transcription regulator recruiting activity; IBA:GO_Central.
GO:0001139; F:RNA polymerase II complex recruiting activity; IBA:GO_Central.
GO:0001162; F:RNA polymerase II intronic transcription regulatory region sequence-specific DNA binding; IEA:Ensembl.
GO:0001164; F:RNA polymerase I core promoter sequence-specific DNA binding; IMP:UniProtKB.
GO:0001165; F:RNA polymerase I cis-regulatory region sequence-specific DNA binding; IDA:UniProtKB.
GO:0001172; P:transcription, RNA-templated; IDA:BHF-UCL.
GO:0001174; P:transcriptional start site selection at RNA polymerase II promoter; IMP:UniProtKB.
GO:0001179; F:RNA polymerase I general transcription initiation factor binding; IEA:Ensembl.
GO:0001181; F:RNA polymerase I general transcription initiation factor activity; IBA:GO_Central.
GO:0001188; P:RNA polymerase I preinitiation complex assembly; IDA:UniProtKB.
GO:0001193; P:maintenance of transcriptional fidelity during DNA-templated transcription elongation from RNA polymerase II promoter; IBA:GO_Central.
GO:0001225; F:RNA polymerase II transcription coactivator binding; IPI:ARUK-UCL.
GO:0001226; F:RNA polymerase II transcription corepressor binding; IDA:UniProtKB.
GO:0001227; F:DNA-binding transcription repressor activity, RNA polymerase II-specific; NAS:BHF-UCL.
GO:0001228; F:DNA-binding transcription activator activity, RNA polymerase II-specific; ISS:UniProtKB.
GO:0001510; P:RNA methylation; ISS:UniProtKB.
GO:0001680; P:tRNA 3'-terminal CCA addition; IDA:UniProtKB.
GO:0001682; P:tRNA 5'-leader removal; IGI:CAFA.
GO:0001734; F:mRNA (N6-adenosine)-methyltransferase activity; IDA:UniProtKB.
GO:0002098; P:tRNA wobble uridine modification; NAS:UniProtKB.
GO:0002100; P:tRNA wobble adenosine to inosine editing; IBA:GO_Central.
GO:0002101; P:tRNA wobble cytosine modification; IDA:UniProtKB.
GO:0002127; P:tRNA wobble base cytosine methylation; IDA:UniProtKB.
GO:0002128; P:tRNA nucleoside ribose methylation; IEA:UniProtKB-UniRule.
GO:0002143; P:tRNA wobble position uridine thiolation; IBA:GO_Central.
GO:0002144; C:cytosolic tRNA wobble base thiouridylase complex; IBA:GO_Central.
GO:0002151; F:G-quadruplex RNA binding; ISS:UniProtKB.
GO:0002153; F:steroid receptor RNA activator RNA binding; IDA:UniProtKB.
GO:0002161; F:aminoacyl-tRNA editing activity; IEA:InterPro.
GO:0002192; P:IRES-dependent translational initiation of linear mRNA; IEA:Ensembl.
GO:0002196; F:Ser-tRNA(Ala) hydrolase activity; ISS:UniProtKB.
GO:0002926; P:tRNA wobble base 5-methoxycarbonylmethyl-2-thiouridinylation; IBA:GO_Central.
GO:0002939; P:tRNA N1-guanine methylation; IBA:GO_Central.
GO:0002940; P:tRNA N2-guanine methylation; IBA:GO_Central.
GO:0002943; P:tRNA dihydrouridine synthesis; IDA:UniProtKB.
GO:0002946; P:tRNA C5-cytosine methylation; IDA:UniProtKB.
GO:0002949; P:tRNA threonylcarbamoyladenosine modification; IEA:UniProtKB-UniRule.
GO:0003256; P:regulation of transcription from RNA polymerase II promoter involved in myocardial precursor cell

differentiation; ISS:BHF-UCL.
GO:0003257; P:positive regulation of transcription from RNA polymerase II promoter involved in myocardial precursor cell differentiation; ISS:BHF-UCL.
GO:0003721; F:telomerase RNA reverse transcriptase activity; IDA:BHF-UCL.
GO:0003723; F:RNA binding; TAS:UniProtKB.
GO:0003724; F:RNA helicase activity; TAS:ProtInc.
GO:0003725; F:double-stranded RNA binding; TAS:ProtInc.
GO:0003726; F:double-stranded RNA adenosine deaminase activity; IDA:MGI.
GO:0003727; F:single-stranded RNA binding; TAS:ProtInc.
GO:0003729; F:mRNA binding; TAS:UniProtKB.
GO:0003730; F:mRNA 3'-UTR binding; TAS:ProtInc.
GO:0003899; F:DNA-directed 5'-3' RNA polymerase activity; TAS:ProtInc.
GO:0003963; F:RNA-3'-phosphate cyclase activity; IBA:GO_Central.
GO:0003964; F:RNA-directed DNA polymerase activity; IEA:UniProtKB-KW.
GO:0003968; F:RNA-directed 5'-3' RNA polymerase activity; IEA:UniProtKB-KW.
GO:0003972; F:RNA ligase (ATP) activity; IDA:UniProtKB.
GO:0004045; F:aminoacyl-tRNA hydrolase activity; IMP:CAFA.
GO:0004479; F:methionyl-tRNA formyltransferase activity; IBA:GO_Central.
GO:0004482; F:mRNA (guanine-N7-)-methyltransferase activity; IDA:UniProtKB.
GO:0004483; F:mRNA (nucleoside-2'-O-)-methyltransferase activity; IDA:UniProtKB.
GO:0004484; F:mRNA guanylyltransferase activity; IDA:UniProtKB.
GO:0004523; F:RNA-DNA hybrid ribonuclease activity; TAS:UniProtKB.
GO:0004549; F:tRNA-specific ribonuclease activity; EXP:Reactome.
GO:0004809; F:tRNA (guanine-N2-)-methyltransferase activity; IBA:GO_Central.
GO:0004813; F:alanine-tRNA ligase activity; IMP:BHF-UCL.
GO:0004814; F:arginine-tRNA ligase activity; IEA:InterPro.
GO:0004815; F:aspartate-tRNA ligase activity; IDA:UniProtKB.
GO:0004816; F:asparagine-tRNA ligase activity; ISS:UniProtKB.
GO:0004817; F:cysteine-tRNA ligase activity; IDA:UniProtKB.
GO:0004818; F:glutamate-tRNA ligase activity; TAS:Reactome.
GO:0004819; F:glutamine-tRNA ligase activity; IDA:UniProtKB.
GO:0004820; F:glycine-tRNA ligase activity; IDA:UniProtKB.
GO:0004821; F:histidine-tRNA ligase activity; IDA:WormBase.
GO:0004822; F:isoleucine-tRNA ligase activity; IDA:UniProtKB.
GO:0004823; F:leucine-tRNA ligase activity; IDA:UniProtKB.
GO:0004824; F:lysine-tRNA ligase activity; IDA:UniProtKB.
GO:0004825; F:methionine-tRNA ligase activity; IDA:UniProtKB.
GO:0004826; F:phenylalanine-tRNA ligase activity; IEA:InterPro.
GO:0004827; F:proline-tRNA ligase activity; IDA:UniProtKB.
GO:0004828; F:serine-tRNA ligase activity; ISS:UniProtKB.
GO:0004829; F:threonine-tRNA ligase activity; ISS:UniProtKB.
GO:0004830; F:tryptophan-tRNA ligase activity; IMP:UniProtKB.
GO:0004831; F:tyrosine-tRNA ligase activity; IDA:BHF-UCL.
GO:0004832; F:valine-tRNA ligase activity; IDA:UniProtKB.
GO:0005665; C:RNA polymerase II, core complex; IEA:InterPro.
GO:0005666; C:RNA polymerase III complex; IDA:UniProtKB.
GO:0005668; C:RNA polymerase transcription factor SL1 complex; IEA:InterPro.
GO:0005736; C:RNA polymerase I complex; IBA:GO_Central.
GO:0005845; C:mRNA cap binding complex; ISS:UniProtKB.
GO:0005847; C:mRNA cleavage and polyadenylation specificity factor complex; IEA:Ensembl.
GO:0005848; C:mRNA cleavage stimulating factor complex; IBA:GO_Central.
GO:0005849; C:mRNA cleavage factor complex; IEA:UniProtKB-UniRule.
GO:0006269; P:DNA replication, synthesis of RNA primer; TAS:ProtInc.
GO:0006278; P:RNA-dependent DNA biosynthetic process; TAS:Reactome.
GO:0006356; P:regulation of transcription by RNA polymerase I; TAS:ProtInc.
GO:0006357; P:regulation of transcription by RNA polymerase II; TAS:UniProtKB.
GO:0006359; P:regulation of transcription by RNA polymerase III; TAS:UniProtKB.
GO:0006360; P:transcription by RNA polymerase I; TAS:ProtInc.
GO:0006361; P:transcription initiation from RNA polymerase I promoter; TAS:Reactome.
GO:0006362; P:transcription elongation from RNA polymerase I promoter; TAS:Reactome.
GO:0006363; P:termination of RNA polymerase I transcription; TAS:Reactome.
GO:0006364; P:rRNA processing; TAS:UniProtKB.
GO:0006366; P:transcription by RNA polymerase II; TAS:UniProtKB.
GO:0006367; P:transcription initiation from RNA polymerase II promoter; TAS:UniProtKB.
GO:0006368; P:transcription elongation from RNA polymerase II promoter; TAS:Reactome.
GO:0006369; P:termination of RNA polymerase II transcription; TAS:Reactome.
GO:0006370; P:7-methylguanosine mRNA capping; TAS:Reactome.
GO:0006376; P:mRNA splice site selection; TAS:ProtInc.
GO:0006378; P:mRNA polyadenylation; TAS:UniProtKB.

GO:0006379; P:mRNA cleavage; TAS:ProtInc.
GO:0006383; P:transcription by RNA polymerase III; TAS:ProtInc.
GO:0006384; P:transcription initiation from RNA polymerase III promoter; TAS:ProtInc.
GO:0006386; P:termination of RNA polymerase III transcription; IBA:GO_Central.
GO:0006388; P:tRNA splicing, via endonucleolytic cleavage and ligation; TAS:Reactome.
GO:0006396; P:RNA processing; TAS:UniProtKB.
GO:0006397; P:mRNA processing; TAS:UniProtKB.
GO:0006398; P:mRNA 3'-end processing by stem-loop binding and cleavage; ISS:UniProtKB.
GO:0006399; P:tRNA metabolic process; IBA:GO_Central.
GO:0006400; P:tRNA modification; TAS:UniProtKB.
GO:0006401; P:RNA catabolic process; TAS:ProtInc.
GO:0006402; P:mRNA catabolic process; TAS:ParkinsonsUK-UCL.
GO:0006403; P:RNA localization; IMP:MGI.
GO:0006404; P:RNA import into nucleus; IDA:UniProtKB.
GO:0006405; P:RNA export from nucleus; TAS:Reactome.
GO:0006406; P:mRNA export from nucleus; TAS:UniProtKB.
GO:0006407; P:rRNA export from nucleus; IMP:UniProtKB.
GO:0006408; P:snRNA export from nucleus; ISS:UniProtKB.
GO:0006409; P:tRNA export from nucleus; TAS:Reactome.
GO:0006418; P:tRNA aminoacylation for protein translation; TAS:Reactome.
GO:0006419; P:alanyl-tRNA aminoacylation; IEA:InterPro.
GO:0006420; P:arginyl-tRNA aminoacylation; IEA:InterPro.
GO:0006421; P:asparaginyl-tRNA aminoacylation; ISS:UniProtKB.
GO:0006422; P:aspartyl-tRNA aminoacylation; IBA:GO_Central.
GO:0006423; P:cysteinyl-tRNA aminoacylation; IDA:UniProtKB.
GO:0006424; P:glutamyl-tRNA aminoacylation; IEA:InterPro.
GO:0006425; P:glutaminyl-tRNA aminoacylation; IDA:UniProtKB.
GO:0006426; P:glycyl-tRNA aminoacylation; IBA:GO_Central.
GO:0006427; P:histidyl-tRNA aminoacylation; IDA:WormBase.
GO:0006428; P:isoleucyl-tRNA aminoacylation; IDA:UniProtKB.
GO:0006429; P:leucyl-tRNA aminoacylation; IDA:HGNC.
GO:0006430; P:lysyl-tRNA aminoacylation; IDA:UniProtKB.
GO:0006431; P:methionyl-tRNA aminoacylation; IDA:UniProtKB.
GO:0006432; P:phenylalanyl-tRNA aminoacylation; IDA:UniProtKB.
GO:0006433; P:prolyl-tRNA aminoacylation; IDA:UniProtKB.
GO:0006434; P:seryl-tRNA aminoacylation; ISS:UniProtKB.
GO:0006435; P:threonyl-tRNA aminoacylation; ISS:UniProtKB.
GO:0006436; P:tryptophanyl-tRNA aminoacylation; IBA:GO_Central.
GO:0006437; P:tyrosyl-tRNA aminoacylation; TAS:ProtInc.
GO:0006438; P:valyl-tRNA aminoacylation; IBA:GO_Central.
GO:0006990; P:positive regulation of transcription from RNA polymerase II promoter involved in unfolded protein response; ISS:UniProtKB.
GO:0008033; P:tRNA processing; TAS:ProtInc.
GO:0008097; F:5S rRNA binding; IMP:CAFA.
GO:0008135; F:translation factor activity, RNA binding; TAS:UniProtKB.
GO:0008173; F:RNA methyltransferase activity; TAS:Reactome.
GO:0008175; F:tRNA methyltransferase activity; IDA:UniProtKB.
GO:0008176; F:tRNA (guanine-N7-)-methyltransferase activity; IDA:UniProtKB.
GO:0008186; F:RNA-dependent ATPase activity; TAS:ProtInc.
GO:0008192; F:RNA guanylyltransferase activity; IDA:UniProtKB.
GO:0008193; F:tRNA guanylyltransferase activity; IDA:UniProtKB.
GO:0008251; F:tRNA-specific adenosine deaminase activity; IMP:UniProtKB.
GO:0008266; F:poly(U) RNA binding; TAS:ProtInc.
GO:0008298; P:intracellular mRNA localization; NAS:UniProtKB.
GO:0008312; F:7S RNA binding; TAS:ProtInc.
GO:0008334; P:histone mRNA metabolic process; TAS:Reactome.
GO:0008353; F:RNA polymerase II CTD heptapeptide repeat kinase activity; ISS:UniProtKB.
GO:0008380; P:RNA splicing; TAS:UniProtKB.
GO:0008419; F:RNA lariat debranching enzyme activity; IMP:UniProtKB.
GO:0008420; F:RNA polymerase II CTD heptapeptide repeat phosphatase activity; IMP:UniProtKB.
GO:0008479; F:queuine tRNA-ribosyltransferase activity; IEA:UniProtKB-UniRule.
GO:0008649; F:rRNA methyltransferase activity; IBA:GO_Central.
GO:0008650; F:rRNA (uridine-2'-O-)-methyltransferase activity; IBA:GO_Central.
GO:0008988; F:rRNA (adenine-N6-)-methyltransferase activity; IDA:UniProtKB.
GO:0009019; F:tRNA (guanine-N1-)-methyltransferase activity; IDA:CAFA.
GO:0009020; F:tRNA (guanosine-2'-O-)-methyltransferase activity; EXP:Reactome.
GO:0009299; P:mRNA transcription; IMP:UniProtKB.
GO:0009301; P:snRNA transcription; TAS:ProtInc.
GO:0009303; P:rRNA transcription; TAS:ProtInc.

GO:0009304; P:tRNA transcription; TAS:ProtInc.
GO:0009328; C:phenylalanine-tRNA ligase complex; IDA:UniProtKB.
GO:0009383; F:rRNA (cytosine-C5-)-methyltransferase activity; IBA:GO_Central.
GO:0009451; P:RNA modification; TAS:ProtInc.
GO:0009452; P:7-methylguanosine RNA capping; IEA:InterPro.
GO:0010501; P:RNA secondary structure unwinding; IDA:UniProtKB.
GO:0010526; P:negative regulation of transposition, RNA-mediated; IDA:UniProtKB.
GO:0010586; P:miRNA metabolic process; TAS:Reactome.
GO:0010587; P:miRNA catabolic process; IMP:UniProtKB.
GO:0010603; P:regulation of cytoplasmic mRNA processing body assembly; IDA:UniProtKB.
GO:0010606; P:positive regulation of cytoplasmic mRNA processing body assembly; IMP:UniProtKB.
GO:0010607; P:negative regulation of cytoplasmic mRNA processing body assembly; IEA:Ensembl.
GO:0010609; P:mRNA localization resulting in posttranscriptional regulation of gene expression; NAS:BHF-UCL.
GO:0010610; P:regulation of mRNA stability involved in response to stress; IMP:UniProtKB.
GO:0010767; P:regulation of transcription from RNA polymerase II promoter in response to UV-induced DNA damage; ISS:UniProtKB.
GO:0010768; P:negative regulation of transcription from RNA polymerase II promoter in response to UV-induced DNA damage; IMP:ParkinsonsUK-UCL.
GO:0010793; P:regulation of mRNA export from nucleus; ISS:UniProtKB.
GO:0016031; P:tRNA import into mitochondrion; IBA:GO_Central.
GO:0016070; P:RNA metabolic process; TAS:UniProtKB.
GO:0016071; P:mRNA metabolic process; NAS:UniProtKB.
GO:0016072; P:rRNA metabolic process; TAS:ARUK-UCL.
GO:0016073; P:snRNA metabolic process; IDA:UniProtKB.
GO:0016075; P:rRNA catabolic process; NAS:UniProtKB.
GO:0016076; P:snRNA catabolic process; ISS:UniProtKB.
GO:0016077; P:snoRNA catabolic process; IDA:UniProtKB.
GO:0016078; P:tRNA catabolic process; IDA:UniProtKB.
GO:0016180; P:snRNA processing; IMP:UniProtKB.
GO:0016246; P:RNA interference; NAS:UniProtKB.
GO:0016251; F:RNA polymerase II general transcription initiation factor activity; IMP:UniProtKB.
GO:0016300; F:tRNA (uracil) methyltransferase activity; IDA:UniProtKB.
GO:0016422; F:mRNA (2'-O-methyladenosine-N6-)-methyltransferase activity; IEA:InterPro.
GO:0016423; F:tRNA (guanine) methyltransferase activity; IBA:GO_Central.
GO:0016427; F:tRNA (cytosine) methyltransferase activity; ISS:UniProtKB.
GO:0016428; F:tRNA (cytosine-5-)-methyltransferase activity; IDA:UniProtKB.
GO:0016429; F:tRNA (adenine-N1-)-methyltransferase activity; IEA:InterPro.
GO:0016430; F:tRNA (adenine-N6-)-methyltransferase activity; IDA:UniProtKB.
GO:0016433; F:rRNA (adenine) methyltransferase activity; IMP:UniProtKB.
GO:0016435; F:rRNA (guanine) methyltransferase activity; IMP:UniProtKB.
GO:0016479; P:negative regulation of transcription by RNA polymerase I; IDA:CACAO.
GO:0016480; P:negative regulation of transcription by RNA polymerase III; IDA:UniProtKB.
GO:0016556; P:mRNA modification; IEA:InterPro.
GO:0016591; C:RNA polymerase II, holoenzyme; IEA:InterPro.
GO:0016973; P:poly(A)+ mRNA export from nucleus; IMP:UniProtKB.
GO:0017055; P:negative regulation of RNA polymerase II transcriptional preinitiation complex assembly; IDA:UniProtKB.
GO:0017069; F:snRNA binding; IDA:UniProtKB.
GO:0017070; F:U6 snRNA binding; NAS:UniProtKB.
GO:0017101; C:aminoacyl-tRNA synthetase multienzyme complex; IDA:UniProtKB.
GO:0017130; F:poly(C) RNA binding; IDA:UniProtKB.
GO:0017150; F:tRNA dihydrouridine synthase activity; IDA:UniProtKB.
GO:0017151; F:DEAD/H-box RNA helicase binding; TAS:UniProtKB.
GO:0019074; P:viral RNA genome packaging; IMP:CACAO.
GO:0019185; C:snRNA-activating protein complex; IDA:UniProtKB.
GO:0019843; F:rRNA binding; TAS:UniProtKB.
GO:0021882; P:regulation of transcription from RNA polymerase II promoter involved in forebrain neuron fate commitment; IEA:Ensembl.
GO:0021912; P:regulation of transcription from RNA polymerase II promoter involved in spinal cord motor neuron fate specification; IEA:Ensembl.
GO:0021913; P:regulation of transcription from RNA polymerase II promoter involved in ventral spinal cord interneuron specification; IEA:Ensembl.
GO:0021918; P:regulation of transcription from RNA polymerase II promoter involved in somatic motor neuron fate commitment; IEA:Ensembl.
GO:0021920; P:regulation of transcription from RNA polymerase II promoter involved in spinal cord association neuron specification; IEA:Ensembl.
GO:0030422; P:production of siRNA involved in RNA interference; TAS:Reactome.
GO:0030423; P:targeting of mRNA for destruction involved in RNA interference; IMP:UniProtKB.
GO:0030488; P:tRNA methylation; ISS:UniProtKB.
GO:0030490; P:maturation of SSU-rRNA; ISS:UniProtKB.

GO:0030515; F:snoRNA binding; ISS:UniProtKB.
GO:0030619; F:U1 snRNA binding; IDA:UniProtKB.
GO:0030620; F:U2 snRNA binding; IEA:Ensembl.
GO:0030621; F:U4 snRNA binding; IDA:UniProtKB.
GO:0030622; F:U4atac snRNA binding; IDA:UniProtKB.
GO:0030623; F:U5 snRNA binding; IBA:GO_Central.
GO:0030624; F:U6atac snRNA binding; IDA:UniProtKB.
GO:0030626; F:U12 snRNA binding; IBA:GO_Central.
GO:0030627; F:pre-mRNA 5'-splice site binding; IBA:GO_Central.
GO:0030628; F:pre-mRNA 3'-splice site binding; IDA:UniProtKB.
GO:0030629; F:U6 snRNA 3'-end binding; IDA:UniProtKB.
GO:0030697; F:S-adenosylmethionine-dependent tRNA (m5U54) methyltransferase activity; IEA:UniProtKB-EC.
GO:0030895; C:apolipoprotein B mRNA editing enzyme complex; TAS:HGNC-UCL.
GO:0030956; C:glutamyl-tRNA(Gln) amidotransferase complex; IDA:UniProtKB.
GO:0031047; P:gene silencing by RNA; ISS:UniProtKB.
GO:0031048; P:chromatin silencing by small RNA; IBA:GO_Central.
GO:0031053; P:primary miRNA processing; TAS:BHF-UCL.
GO:0031054; P:pre-miRNA processing; IMP:UniProtKB.
GO:0031086; P:nuclear-transcribed mRNA catabolic process, deadenylation-independent decay; ISS:UniProtKB.
GO:0031087; P:deadenylation-independent decapping of nuclear-transcribed mRNA; TAS:UniProtKB.
GO:0031118; P:rRNA pseudouridine synthesis; TAS:Reactome.
GO:0031119; P:tRNA pseudouridine synthesis; IMP:UniProtKB.
GO:0031120; P:snRNA pseudouridine synthesis; IBA:GO_Central.
GO:0031123; P:RNA 3'-end processing; IMP:UniProtKB.
GO:0031124; P:mRNA 3'-end processing; TAS:UniProtKB.
GO:0031125; P:rRNA 3'-end processing; ISS:UniProtKB.
GO:0031167; P:rRNA methylation; TAS:Reactome.
GO:0031379; C:RNA-directed RNA polymerase complex; IPI:BHF-UCL.
GO:0031380; C:nuclear RNA-directed RNA polymerase complex; IC:UniProtKB.
GO:0031439; P:positive regulation of mRNA cleavage; IDA:UniProtKB.
GO:0031440; P:regulation of mRNA 3'-end processing; IDA:UniProtKB.
GO:0031441; P:negative regulation of mRNA 3'-end processing; NAS:UniProtKB.
GO:0031442; P:positive regulation of mRNA 3'-end processing; IMP:UniProtKB.
GO:0031515; C:tRNA (m1A) methyltransferase complex; IBA:GO_Central.
GO:0031533; C:mRNA cap methyltransferase complex; IDA:UniProtKB.
GO:0031990; P:mRNA export from nucleus in response to heat stress; IDA:UniProtKB.
GO:0032197; P:transposition, RNA-mediated; IMP:UniProtKB.
GO:0032199; P:reverse transcription involved in RNA-mediated transposition; IDA:UniProtKB.
GO:0032574; F:5'-3' RNA helicase activity; IDA:UniProtKB.
GO:0032968; P:positive regulation of transcription elongation from RNA polymerase II promoter; ISS:UniProtKB.
GO:0033119; P:negative regulation of RNA splicing; IDA:UniProtKB.
GO:0033120; P:positive regulation of RNA splicing; IMP:UniProtKB.
GO:0033168; P:conversion of ds siRNA to ss siRNA involved in RNA interference; IMP:BHF-UCL.
GO:0033204; F:ribonuclease P RNA binding; IDA:UniProtKB.
GO:0033227; P:dsRNA transport; IMP:UniProtKB.
GO:0033592; F:RNA strand annealing activity; IEA:InterPro.
GO:0033677; F:DNA/RNA helicase activity; IDA:UniProtKB.
GO:0033678; F:5'-3' DNA/RNA helicase activity; IDA:BHF-UCL.
GO:0033679; F:3'-5' DNA/RNA helicase activity; IDA:UniProtKB.
GO:0033962; P:cytoplasmic mRNA processing body assembly; ISS:BHF-UCL.
GO:0033979; P:box H/ACA snoRNA metabolic process; IEA:Ensembl.
GO:0034062; F:5'-3' RNA polymerase activity; TAS:Reactome.
GO:0034227; P:tRNA thio-modification; NAS:UniProtKB.
GO:0034243; P:regulation of transcription elongation from RNA polymerase II promoter; ISS:UniProtKB.
GO:0034244; P:negative regulation of transcription elongation from RNA polymerase II promoter; ISS:UniProtKB.
GO:0034245; C:mitochondrial DNA-directed RNA polymerase complex; IBA:GO_Central.
GO:0034247; P:snoRNA splicing; IBA:GO_Central.
GO:0034337; P:RNA folding; IDA:UniProtKB.
GO:0034353; F:RNA pyrophosphohydrolase activity; ISS:UniProtKB.
GO:0034395; P:regulation of transcription from RNA polymerase II promoter in response to iron; IEA:Ensembl.
GO:0034402; P:recruitment of 3'-end processing factors to RNA polymerase II holoenzyme complex; IBA:GO_Central.
GO:0034427; P:nuclear-transcribed mRNA catabolic process, exonucleolytic, 3'-5'; IEA:InterPro.
GO:0034458; F:3'-5' RNA helicase activity; IDA:UniProtKB.
GO:0034472; P:snRNA 3'-end processing; IMP:UniProtKB.
GO:0034473; P:U1 snRNA 3'-end processing; IBA:GO_Central.
GO:0034474; P:U2 snRNA 3'-end processing; IBA:GO_Central.
GO:0034475; P:U4 snRNA 3'-end processing; IBA:GO_Central.
GO:0034476; P:U5 snRNA 3'-end processing; IBA:GO_Central.
GO:0034477; P:U6 snRNA 3'-end processing; IMP:UniProtKB.

GO:0034511; F:U3 snoRNA binding; IEA:InterPro.
GO:0034512; F:box C/D snoRNA binding; IEA:Ensembl.
GO:0034513; F:box H/ACA snoRNA binding; IPI:BHF-UCL.
GO:0034518; C:RNA cap binding complex; TAS:UniProtKB.
GO:0034584; F:piRNA binding; ISS:UniProtKB.
GO:0034587; P:piRNA metabolic process; ISS:UniProtKB.
GO:0035087; P:siRNA loading onto RISC involved in RNA interference; IDA:UniProtKB.
GO:0035194; P:posttranscriptional gene silencing by RNA; TAS:Reactome.
GO:0035195; P:gene silencing by miRNA; TAS:UniProtKB.
GO:0035196; P:production of miRNAs involved in gene silencing by miRNA; IMP:UniProtKB.
GO:0035197; F:siRNA binding; ISS:UniProtKB.
GO:0035198; F:miRNA binding; ISS:UniProtKB.
GO:0035278; P:miRNA mediated inhibition of translation; TAS:UniProtKB.
GO:0035279; P:mRNA cleavage involved in gene silencing by miRNA; IDA:UniProtKB.
GO:0035280; P:miRNA loading onto RISC involved in gene silencing by miRNA; IDA:MGI.
GO:0035281; P:pre-miRNA export from nucleus; IDA:BHF-UCL.
GO:0035513; P:oxidative RNA demethylation; IDA:UniProtKB.
GO:0035515; F:oxidative RNA demethylase activity; IMP:UniProtKB.
GO:0035553; P:oxidative single-stranded RNA demethylation; IDA:UniProtKB.
GO:0035600; P:tRNA methylthiolation; IBA:GO_Central.
GO:0035613; F:RNA stem-loop binding; ISS:UniProtKB.
GO:0035925; F:mRNA 3'-UTR AU-rich region binding; ISS:UniProtKB.
GO:0035927; P:RNA import into mitochondrion; IDA:UniProtKB.
GO:0035928; P:rRNA import into mitochondrion; IMP:UniProtKB.
GO:0035945; P:mitochondrial ncRNA surveillance; IMP:UniProtKB.
GO:0035946; P:mitochondrial mRNA surveillance; IMP:UniProtKB.
GO:0035947; P:regulation of gluconeogenesis by regulation of transcription from RNA polymerase II promoter; ISS:UniProtKB.
GO:0035948; P:positive regulation of gluconeogenesis by positive regulation of transcription from RNA polymerase II promoter; IEA:Ensembl.
GO:0036002; F:pre-mRNA binding; TAS:BHF-UCL.
GO:0036003; P:positive regulation of transcription from RNA polymerase II promoter in response to stress; ISS:UniProtKB.
GO:0036031; P:recruitment of mRNA capping enzyme to RNA polymerase II holoenzyme complex; IDA:UniProtKB.
GO:0036091; P:positive regulation of transcription from RNA polymerase II promoter in response to oxidative stress; IMP:UniProtKB.
GO:0036265; P:RNA (guanine-N7)-methylation; IBA:GO_Central.
GO:0036317; F:tyrosyl-RNA phosphodiesterase activity; IDA:UniProtKB.
GO:0036396; C:RNA N6-methyladenosine methyltransferase complex; IDA:UniProtKB.
GO:0036404; P:conversion of ds siRNA to ss siRNA; IMP:AgBase.
GO:0036416; P:tRNA stabilization; ISS:UniProtKB.
GO:0039689; P:negative stranded viral RNA replication; IEA:Ensembl.
GO:0039692; P:single stranded viral RNA replication via double stranded DNA intermediate; IDA:MGI.
GO:0039694; P:viral RNA genome replication; IMP:ParkinsonsUK-UCL.
GO:0040031; P:snRNA modification; IDA:UniProtKB.
GO:0042134; F:rRNA primary transcript binding; IDA:UniProtKB.
GO:0042245; P:RNA repair; IDA:UniProtKB.
GO:0042272; C:nuclear RNA export factor complex; NAS:UniProtKB.
GO:0042565; C:RNA nuclear export complex; IDA:BHF-UCL.
GO:0042779; P:tRNA 3'-trailer cleavage; IEA:InterPro.
GO:0042780; P:tRNA 3'-end processing; TAS:Reactome.
GO:0042781; F:3'-tRNA processing endoribonuclease activity; IBA:GO_Central.
GO:0042789; P:mRNA transcription by RNA polymerase II; TAS:BHF-UCL.
GO:0042790; P:nucleolar large rRNA transcription by RNA polymerase I; IBA:GO_Central.
GO:0042791; P:5S class rRNA transcription by RNA polymerase III; IC:HGNC-UCL.
GO:0042795; P:snRNA transcription by RNA polymerase II; TAS:Reactome.
GO:0042796; P:snRNA transcription by RNA polymerase III; IMP:UniProtKB.
GO:0042797; P:tRNA transcription by RNA polymerase III; IC:HGNC-UCL.
GO:0043039; P:tRNA aminoacylation; IDA:BHF-UCL.
GO:0043137; P:DNA replication, removal of RNA primer; IDA:UniProtKB.
GO:0043175; F:RNA polymerase core enzyme binding; IPI:UniProtKB.
GO:0043330; P:response to exogenous dsRNA; ISS:UniProtKB.
GO:0043331; P:response to dsRNA; IEA:Ensembl.
GO:0043484; P:regulation of RNA splicing; ISS:UniProtKB.
GO:0043488; P:regulation of mRNA stability; TAS:Reactome.
GO:0043489; P:RNA stabilization; ISS:BHF-UCL.
GO:0043527; C:tRNA methyltransferase complex; IDA:UniProtKB.
GO:0043618; P:regulation of transcription from RNA polymerase II promoter in response to stress; IDA:BHF-UCL.
GO:0043619; P:regulation of transcription from RNA polymerase II promoter in response to oxidative stress; ISS:BHF-UCL.
GO:0043629; P:ncRNA polyadenylation; IDA:UniProtKB.
GO:0043630; P:ncRNA polyadenylation involved in polyadenylation-dependent ncRNA catabolic process; IMP:BHF-UCL.

GO:0043631; P:RNA polyadenylation; ISS:UniProtKB.
GO:0043928; P:exonucleolytic catabolism of deadenylated mRNA; TAS:Reactome.
GO:0044377; F:RNA polymerase II cis-regulatory region sequence-specific DNA binding, bending; IEA:Ensembl.
GO:0044528; P:regulation of mitochondrial mRNA stability; IMP:UniProtKB.
GO:0044830; P:modulation by host of viral RNA genome replication; IMP:UniProtKB.
GO:0045091; P:regulation of single stranded viral RNA replication via double stranded DNA intermediate; IDA:UniProtKB.
GO:0045131; F:pre-mRNA branch point binding; IEA:InterPro.
GO:0045292; P:mRNA cis splicing, via spliceosome; IEA:InterPro.
GO:0045869; P:negative regulation of single stranded viral RNA replication via double stranded DNA intermediate; ISS:UniProtKB.
GO:0045870; P:positive regulation of single stranded viral RNA replication via double stranded DNA intermediate; IMP:UniProtKB.
GO:0045898; P:regulation of RNA polymerase II transcriptional preinitiation complex assembly; IDA:UniProtKB.
GO:0045899; P:positive regulation of RNA polymerase II transcriptional preinitiation complex assembly; IEA:Ensembl.
GO:0045943; P:positive regulation of transcription by RNA polymerase I; ISS:UniProtKB.
GO:0045944; P:positive regulation of transcription by RNA polymerase II; TAS:UniProtKB.
GO:0045945; P:positive regulation of transcription by RNA polymerase III; IMP:UniProtKB.
GO:0046778; P:modification by virus of host mRNA processing; TAS:Reactome.
GO:0046784; P:viral mRNA export from host cell nucleus; IDA:UniProtKB.
GO:0046831; P:regulation of RNA export from nucleus; ISS:UniProtKB.
GO:0046832; P:negative regulation of RNA export from nucleus; IDA:UniProtKB.
GO:0046833; P:positive regulation of RNA export from nucleus; ISS:UniProtKB.
GO:0048024; P:regulation of mRNA splicing, via spliceosome; TAS:UniProtKB.
GO:0048025; P:negative regulation of mRNA splicing, via spliceosome; ISS:UniProtKB.
GO:0048026; P:positive regulation of mRNA splicing, via spliceosome; ISS:UniProtKB.
GO:0048027; F:mRNA 5'-UTR binding; IMP:CAFA.
GO:0048254; P:snoRNA localization; IMP:UniProtKB.
GO:0048255; P:mRNA stabilization; TAS:UniProtKB.
GO:0050265; F:RNA uridylyltransferase activity; IDA:UniProtKB.
GO:0050560; F:aspartate-tRNA(Asn) ligase activity; IDA:BHF-UCL.
GO:0050561; F:glutamate-tRNA(Gln) ligase activity; IDA:UniProtKB.
GO:0050567; F:glutaminyl-tRNA synthase (glutamine-hydrolyzing) activity; IDA:UniProtKB.
GO:0050658; P:RNA transport; TAS:UniProtKB.
GO:0050684; P:regulation of mRNA processing; ISS:UniProtKB.
GO:0050779; P:RNA destabilization; ISS:UniProtKB.
GO:0051028; P:mRNA transport; ISS:UniProtKB.
GO:0051029; P:rRNA transport; IDA:UniProtKB.
GO:0051031; P:tRNA transport; IMP:UniProtKB.
GO:0051033; F:RNA transmembrane transporter activity; IEA:InterPro.
GO:0051123; P:RNA polymerase II preinitiation complex assembly; ISS:BHF-UCL.
GO:0051252; P:regulation of RNA metabolic process; NAS:UniProtKB.
GO:0051391; P:tRNA acetylation; IEA:UniProtKB-UniRule.
GO:0051500; F:D-tyrosyl-tRNA(Tyr) deacylase activity; IBA:GO_Central.
GO:0052381; F:tRNA dimethylallyltransferase activity; EXP:Reactome.
GO:0052666; F:tRNA (cytosine-2'-O-)-methyltransferase activity; EXP:Reactome.
GO:0052717; F:tRNA-specific adenosine-34 deaminase activity; IBA:GO_Central.
GO:0052718; C:tRNA-specific adenosine-34 deaminase complex; IBA:GO_Central.
GO:0052735; F:tRNA (cytosine-3-)-methyltransferase activity; IEA:Ensembl.
GO:0052905; F:tRNA (guanine(9)-N(1))-methyltransferase activity; IEA:UniProtKB-EC.
GO:0052906; F:tRNA (guanine(37)-N(1))-methyltransferase activity; IEA:UniProtKB-EC.
GO:0052907; F:23S rRNA (adenine(1618)-N(6))-methyltransferase activity; IBA:GO_Central.
GO:0052909; F:18S rRNA (adenine(1779)-N(6)/adenine(1780)-N(6))-dimethyltransferase activity; IEA:UniProtKB-EC.
GO:0052927; F:CTP:tRNA cytidylyltransferase activity; IEA:UniProtKB-EC.
GO:0052928; F:CTP:3'-cytidine-tRNA cytidylyltransferase activity; IEA:UniProtKB-EC.
GO:0052929; F:ATP:3'-cytidine-cytidine-tRNA adenylyltransferase activity; IDA:UniProtKB.
GO:0060212; P:negative regulation of nuclear-transcribed mRNA poly(A) tail shortening; IMP:UniProtKB.
GO:0060213; P:positive regulation of nuclear-transcribed mRNA poly(A) tail shortening; ISS:UniProtKB.
GO:0060260; P:regulation of transcription initiation from RNA polymerase II promoter; NAS:ParkinsonsUK-UCL.
GO:0060261; P:positive regulation of transcription initiation from RNA polymerase II promoter; ISS:BHF-UCL.
GO:0060633; P:negative regulation of transcription initiation from RNA polymerase II promoter; IMP:UniProtKB.
GO:0060735; P:regulation of eIF2 alpha phosphorylation by dsRNA; IDA:UniProtKB.
GO:0060807; P:regulation of transcription from RNA polymerase II promoter involved in definitive endodermal cell fate specification; ISS:BHF-UCL.
GO:0060964; P:regulation of gene silencing by miRNA; TAS:UniProtKB.
GO:0060965; P:negative regulation of gene silencing by miRNA; IMP:UniProtKB.
GO:0060994; P:regulation of transcription from RNA polymerase II promoter involved in kidney development; IEA:Ensembl.
GO:0061014; P:positive regulation of mRNA catabolic process; ISS:UniProtKB.
GO:0061015; P:snRNA import into nucleus; IMP:UniProtKB.
GO:0061157; P:mRNA destabilization; NAS:BHF-UCL.

GO:0061158; P:3'-UTR-mediated mRNA destabilization; ISS:UniProtKB.
GO:0061394; P:regulation of transcription from RNA polymerase II promoter in response to arsenic-containing substance; TAS:ParkinsonsUK-UCL.
GO:0061395; P:positive regulation of transcription from RNA polymerase II promoter in response to arsenic-containing substance; TAS:ParkinsonsUK-UCL.
GO:0061396; P:regulation of transcription from RNA polymerase II promoter in response to copper ion; IEA:Ensembl.
GO:0061400; P:positive regulation of transcription from RNA polymerase II promoter in response to calcium ion; IDA:UniProtKB.
GO:0061402; P:positive regulation of transcription from RNA polymerase II promoter in response to acidic pH; IEA:Ensembl.
GO:0061408; P:positive regulation of transcription from RNA polymerase II promoter in response to heat stress; IDA:UniProtKB.
GO:0061418; P:regulation of transcription from RNA polymerase II promoter in response to hypoxia; TAS:Reactome.
GO:0061419; P:positive regulation of transcription from RNA polymerase II promoter in response to hypoxia; ISS:UniProtKB.
GO:0061428; P:negative regulation of transcription from RNA polymerase II promoter in response to hypoxia; IMP:UniProtKB.
GO:0061614; P:pri-miRNA transcription by RNA polymerase II; ISS:UniProtKB.
GO:0061629; F:RNA polymerase II-specific DNA-binding transcription factor binding; ISS:BHF-UCL.
GO:0061632; F:RNA lariat debranching enzyme activator activity; IBA:GO_Central.
GO:0061712; F:tRNA (N(6)-L-threonylcarbamoyladenosine(37)-C(2))-methylthiotransferase; IEA:UniProtKB-EC.
GO:0061715; P:miRNA 2'-O-methylation; IDA:UniProtKB.
GO:0061752; F:telomeric repeat-containing RNA binding; IDA:BHF-UCL.
GO:0061953; F:mRNA (adenine-N1-)-methyltransferase activity; IDA:UniProtKB.
GO:0061987; P:negative regulation of transcription from RNA polymerase II promoter by glucose; ISS:BHF-UCL.
GO:0062103; P:double-stranded RNA biosynthetic process; IDA:ARUK-UCL.
GO:0062105; F:RNA 2'-O-methyltransferase activity; IDA:UniProtKB.
GO:0062152; F:mRNA (cytidine-5-)-methyltransferase activity; IDA:UniProtKB.
GO:0062153; F:C5-methylcytidine-containing RNA binding; IDA:UniProtKB.
GO:0070034; F:telomerase RNA binding; ISS:BHF-UCL.
GO:0070037; F:rRNA (pseudouridine) methyltransferase activity; IDA:UniProtKB.
GO:0070039; F:rRNA (guanosine-2'-O-)-methyltransferase activity; EXP:Reactome.
GO:0070042; F:rRNA (uridine-N3-)-methyltransferase activity; IBA:GO_Central.
GO:0070054; P:mRNA splicing, via endonucleolytic cleavage and ligation; IDA:UniProtKB.
GO:0070063; F:RNA polymerase binding; ISS:UniProtKB.
GO:0070127; P:tRNA aminoacylation for mitochondrial protein translation; IDA:UniProtKB.
GO:0070143; P:mitochondrial alanyl-tRNA aminoacylation; IMP:BHF-UCL.
GO:0070145; P:mitochondrial asparaginyl-tRNA aminoacylation; IDA:UniProtKB.
GO:0070150; P:mitochondrial glycyl-tRNA aminoacylation; IBA:GO_Central.
GO:0070158; P:mitochondrial seryl-tRNA aminoacylation; IBA:GO_Central.
GO:0070159; P:mitochondrial threonyl-tRNA aminoacylation; TAS:BHF-UCL.
GO:0070180; F:large ribosomal subunit rRNA binding; IBA:GO_Central.
GO:0070181; F:small ribosomal subunit rRNA binding; IEA:Ensembl.
GO:0070183; P:mitochondrial tryptophanyl-tRNA aminoacylation; IBA:GO_Central.
GO:0070184; P:mitochondrial tyrosyl-tRNA aminoacylation; IMP:BHF-UCL.
GO:0070329; P:tRNA seleno-modification; IBA:GO_Central.
GO:0070475; P:rRNA base methylation; IBA:GO_Central.
GO:0070476; P:rRNA (guanine-N7)-methylation; IMP:UniProtKB.
GO:0070478; P:nuclear-transcribed mRNA catabolic process, 3'-5' exonucleolytic nonsense-mediated decay; IBA:GO_Central.
GO:0070481; P:nuclear-transcribed mRNA catabolic process, non-stop decay; IEA:InterPro.
GO:0070525; P:tRNA threonylcarbamoyladenosine metabolic process; IBA:GO_Central.
GO:0070551; F:endoribonuclease activity, cleaving siRNA-paired mRNA; IDA:UniProtKB.
GO:0070651; P:nonfunctional rRNA decay; IBA:GO_Central.
GO:0070681; P:glutaminyl-tRNAGln biosynthesis via transamidation; IDA:UniProtKB.
GO:0070816; P:phosphorylation of RNA polymerase II C-terminal domain; IMP:UniProtKB.
GO:0070860; C:RNA polymerase I core factor complex; IDA:UniProtKB.
GO:0070878; F:primary miRNA binding; ISS:BHF-UCL.
GO:0070883; F:pre-miRNA binding; ISS:UniProtKB.
GO:0070898; P:RNA polymerase III preinitiation complex assembly; IEA:GOC.
GO:0070899; P:mitochondrial tRNA wobble uridine modification; IBA:GO_Central.
GO:0070900; P:mitochondrial tRNA modification; TAS:Reactome.
GO:0070901; P:mitochondrial tRNA methylation; TAS:Reactome.
GO:0070902; P:mitochondrial tRNA pseudouridine synthesis; TAS:Reactome.
GO:0070922; P:small RNA loading onto RISC; IMP:UniProtKB.
GO:0070934; P:CRD-mediated mRNA stabilization; IMP:UniProtKB.
GO:0070935; P:3'-UTR-mediated mRNA stabilization; TAS:UniProtKB.
GO:0070937; C:CRD-mediated mRNA stability complex; IDA:UniProtKB.
GO:0070940; P:dephosphorylation of RNA polymerase II C-terminal domain; IMP:UniProtKB.
GO:0070966; P:nuclear-transcribed mRNA catabolic process, no-go decay; IMP:UniProtKB.
GO:0071008; C:U2-type post-mRNA release spliceosomal complex; IDA:UniProtKB.
GO:0071014; C:post-mRNA release spliceosomal complex; IBA:GO_Central.
GO:0071025; P:RNA surveillance; IEA:InterPro.

GO:0071028; P:nuclear mRNA surveillance; ISS:UniProtKB.
GO:0071033; P:nuclear retention of pre-mRNA at the site of transcription; IBA:GO_Central.
GO:0071035; P:nuclear polyadenylation-dependent rRNA catabolic process; IMP:UniProtKB.
GO:0071036; P:nuclear polyadenylation-dependent snoRNA catabolic process; IBA:GO_Central.
GO:0071037; P:nuclear polyadenylation-dependent snRNA catabolic process; IBA:GO_Central.
GO:0071038; P:nuclear polyadenylation-dependent tRNA catabolic process; IBA:GO_Central.
GO:0071042; P:nuclear polyadenylation-dependent mRNA catabolic process; IDA:UniProtKB.
GO:0071044; P:histone mRNA catabolic process; IMP:UniProtKB.
GO:0071045; P:nuclear histone mRNA catabolic process; IMP:CAFA.
GO:0071048; P:nuclear retention of unspliced pre-mRNA at the site of transcription; IMP:UniProtKB.
GO:0071049; P:nuclear retention of pre-mRNA with aberrant 3'-ends at the site of transcription; IBA:GO_Central.
GO:0071050; P:snoRNA polyadenylation; IDA:UniProtKB.
GO:0071051; P:polyadenylation-dependent snoRNA 3'-end processing; IDA:UniProtKB.
GO:0071076; P:RNA 3' uridylation; ISS:UniProtKB.
GO:0071164; F:RNA trimethylguanosine synthase activity; IDA:BHF-UCL.
GO:0071204; C:histone pre-mRNA 3'end processing complex; ISS:UniProtKB.
GO:0071207; F:histone pre-mRNA stem-loop binding; ISS:UniProtKB.
GO:0071208; F:histone pre-mRNA DCP binding; ISS:UniProtKB.
GO:0071209; F:U7 snRNA binding; IPI:BHF-UCL.
GO:0071359; P:cellular response to dsRNA; IMP:UniProtKB.
GO:0071360; P:cellular response to exogenous dsRNA; TAS:BHF-UCL.
GO:0071424; F:rRNA (cytosine-N4-)-methyltransferase activity; IBA:GO_Central.
GO:0071528; P:tRNA re-export from nucleus; IBA:GO_Central.
GO:0071951; P:conversion of methionyl-tRNA to N-formyl-methionyl-tRNA; IBA:GO_Central.
GO:0072368; P:regulation of lipid transport by negative regulation of transcription from RNA polymerase II promoter; IDA:BHF-UCL.
GO:0072369; P:regulation of lipid transport by positive regulation of transcription from RNA polymerase II promoter; IMP:BHF-UCL.
GO:0072669; C:tRNA-splicing ligase complex; IDA:UniProtKB.
GO:0072684; P:mitochondrial tRNA 3'-trailer cleavage, endonucleolytic; IMP:UniProtKB.
GO:0080009; P:mRNA methylation; IMP:UniProtKB.
GO:0090065; P:regulation of production of siRNA involved in RNA interference; IEA:InterPro.
GO:0090366; P:positive regulation of mRNA modification; IEA:Ensembl.
GO:0090501; P:RNA phosphodiester bond hydrolysis; ISS:UniProtKB.
GO:0090502; P:RNA phosphodiester bond hydrolysis, endonucleolytic; IEA:GOC.
GO:0090503; P:RNA phosphodiester bond hydrolysis, exonucleolytic; ISS:BHF-UCL.
GO:0090571; C:RNA polymerase II transcription repressor complex; IEA:Ensembl.
GO:0090575; C:RNA polymerase II transcription factor complex; ISS:BHF-UCL.
GO:0090615; P:mitochondrial mRNA processing; IMP:UniProtKB.
GO:0090624; F:endoribonuclease activity, cleaving miRNA-paired mRNA; IMP:UniProtKB.
GO:0090625; P:mRNA cleavage involved in gene silencing by siRNA; IDA:BHF-UCL.
GO:0090646; P:mitochondrial tRNA processing; TAS:Reactome.
GO:0090666; P:scaRNA localization to Cajal body; IMP:BHF-UCL.
GO:0090669; P:telomerase RNA stabilization; IMP:BHF-UCL.
GO:0090671; P:telomerase RNA localization to Cajal body; IMP:BHF-UCL.
GO:0097056; P:selenocysteinyl-tRNA(Sec) biosynthetic process; IEA:UniProtKB-UniPathway.
GO:0097157; F:pre-mRNA intronic binding; ISS:UniProtKB.
GO:0097158; F:pre-mRNA intronic pyrimidine-rich binding; IDA:UniProtKB.
GO:0097201; P:negative regulation of transcription from RNA polymerase II promoter in response to stress; ISS:UniProtKB.
GO:0097222; P:mitochondrial mRNA polyadenylation; IMP:UniProtKB.
GO:0097309; P:cap1 mRNA methylation; IDA:UniProtKB.
GO:0097310; P:cap2 mRNA methylation; IDA:UniProtKB.
GO:0097322; F:7SK snRNA binding; IEA:Ensembl.
GO:0097694; P:establishment of RNA localization to telomere; IMP:BHF-UCL.
GO:0097745; P:mitochondrial tRNA 5'-end processing; IDA:UniProtKB.
GO:0098680; F:template-free RNA nucleotidyltransferase; IDA:BHF-UCL.
GO:0098781; P:ncRNA transcription; IEA:Ensembl.
GO:0098787; P:mRNA cleavage involved in mRNA processing; IDA:ParkinsonsUK-UCL.
GO:0098789; P:pre-mRNA cleavage required for polyadenylation; IMP:UniProtKB.
GO:0098808; F:mRNA cap binding; IPI:ParkinsonsUK-UCL.
GO:0099122; F:RNA polymerase II C-terminal domain binding; ISS:UniProtKB.
GO:0101030; P:tRNA-guanine transglycosylation; IDA:UniProtKB.
GO:0102264; F:tRNA-dihydrouridine20 synthase activity; IEA:UniProtKB-EC.
GO:0102521; F:tRNA-4-demethylwyosine synthase activity; IEA:UniProtKB-EC.
GO:0102522; F:tRNA 4-demethylwyosine alpha-amino-alpha-carboxypropyltransferase activity; IEA:UniProtKB-EC.
GO:0102524; F:tRNAPhe (7-(3-amino-3-carboxypropyl)wyosine37-C2)-hydroxylase activity; IEA:UniProtKB-EC.
GO:0106004; P:tRNA (guanine-N7)-methylation; IEA:GOC.
GO:0106005; P:RNA 5'-cap (guanine-N7)-methylation; IEA:InterPro.
GO:0106029; F:tRNA pseudouridine synthase activity; IEA:UniProtKB-EC.

GO:0106050; F:tRNA 2'-O-methyltransferase activity; IEA:InterPro.
GO:0106074; P:aminoacyl-tRNA metabolism involved in translational fidelity; IDA:UniProtKB.
GO:0106105; F:Ala-tRNA(Thr) hydrolase activity; IDA:UniProtKB.
GO:0106162; F:mRNA N-acetyltransferase activity; IDA:UniProtKB.
GO:0110008; P:ncRNA deadenylation; IMP:BHF-UCL.
GO:0110104; P:mRNA alternative polyadenylation; IMP:UniProtKB.
GO:0110152; F:RNA NAD-cap (NAD-forming) hydrolase activity; ISS:UniProtKB.
GO:0110153; F:RNA NAD-cap (NMN-forming) hydrolase activity; ISS:UniProtKB.
GO:0120048; F:U6 snRNA (adenine-(43)-N(6))-methyltransferase activity; IDA:UniProtKB.
GO:0120049; P:snRNA (adenine-N6)-methylation; IDA:UniProtKB.
GO:0140262; F:mRNA cap binding complex binding; IEA:Ensembl.
GO:1900153; P:positive regulation of nuclear-transcribed mRNA catabolic process, deadenylation-dependent decay; ISS:UniProtKB.
GO:1900260; P:negative regulation of RNA-directed 5'-3' RNA polymerase activity; IDA:AgBase.
GO:1900363; P:regulation of mRNA polyadenylation; IMP:UniProtKB.
GO:1900364; P:negative regulation of mRNA polyadenylation; IMP:UniProtKB.
GO:1900365; P:positive regulation of mRNA polyadenylation; ISS:UniProtKB.
GO:1900369; P:negative regulation of RNA interference; IEA:Ensembl.
GO:1900370; P:positive regulation of RNA interference; IDA:BHF-UCL.
GO:1900387; P:negative regulation of cell-cell adhesion by negative regulation of transcription from RNA polymerase II promoter; IMP:BHF-UCL.
GO:1900413; P:positive regulation of phospholipid biosynthetic process by positive regulation of transcription from RNA polymerase II promoter; TAS:ParkinsonsUK-UCL.
GO:1900477; P:negative regulation of G1/S transition of mitotic cell cycle by negative regulation of transcription from RNA polymerase II promoter; IDA:BHF-UCL.
GO:1901227; P:negative regulation of transcription from RNA polymerase II promoter involved in heart development; ISS:BHF-UCL.
GO:1901228; P:positive regulation of transcription from RNA polymerase II promoter involved in heart development; ISS:BHF-UCL.
GO:1901407; P:regulation of phosphorylation of RNA polymerase II C-terminal domain; IDA:UniProtKB.
GO:1901522; P:positive regulation of transcription from RNA polymerase II promoter involved in cellular response to chemical stimulus; TAS:BHF-UCL.
GO:1901581; P:negative regulation of telomeric RNA transcription from RNA pol II promoter; ISS:UniProtKB.
GO:1901582; P:positive regulation of telomeric RNA transcription from RNA pol II promoter; IMP:BHF-UCL.
GO:1901835; P:positive regulation of deadenylation-independent decapping of nuclear-transcribed mRNA; IDA:UniProtKB.
GO:1901837; P:negative regulation of transcription of nucleolar large rRNA by RNA polymerase I; IMP:UniProtKB.
GO:1901838; P:positive regulation of transcription of nucleolar large rRNA by RNA polymerase I; IMP:UniProtKB.
GO:1902064; P:regulation of transcription from RNA polymerase II promoter involved in spermatogenesis; ISS:UniProtKB.
GO:1902369; P:negative regulation of RNA catabolic process; IMP:UniProtKB.
GO:1902373; P:negative regulation of mRNA catabolic process; IMP:CAFA.
GO:1902415; P:regulation of mRNA binding; IEA:Ensembl.
GO:1902416; P:positive regulation of mRNA binding; IPI:ParkinsonsUK-UCL.
GO:1902629; P:regulation of mRNA stability involved in cellular response to UV; IMP:UniProtKB.
GO:1902679; P:negative regulation of RNA biosynthetic process; IEA:Ensembl.
GO:1902680; P:positive regulation of RNA biosynthetic process; IMP:ParkinsonsUK-UCL.
GO:1902894; P:negative regulation of pri-miRNA transcription by RNA polymerase II; ISS:BHF-UCL.
GO:1902895; P:positive regulation of pri-miRNA transcription by RNA polymerase II; ISS:BHF-UCL.
GO:1903025; P:regulation of RNA polymerase II regulatory region sequence-specific DNA binding; IMP:MGI.
GO:1903026; P:negative regulation of RNA polymerase II regulatory region sequence-specific DNA binding; IGI:GO_Central.
GO:1903632; P:positive regulation of aminoacyl-tRNA ligase activity; IEA:Ensembl.
GO:1903634; P:negative regulation of leucine-tRNA ligase activity; IEA:Ensembl.
GO:1903704; P:negative regulation of production of siRNA involved in RNA interference; IDA:BHF-UCL.
GO:1903798; P:regulation of production of miRNAs involved in gene silencing by miRNA; IEA:Ensembl.
GO:1903799; P:negative regulation of production of miRNAs involved in gene silencing by miRNA; IMP:BHF-UCL.
GO:1903800; P:positive regulation of production of miRNAs involved in gene silencing by miRNA; ISS:BHF-UCL.
GO:1903839; P:positive regulation of mRNA 3'-UTR binding; IDA:UniProtKB.
GO:1904582; P:positive regulation of intracellular mRNA localization; ISS:UniProtKB.
GO:1904812; P:rRNA acetylation involved in maturation of SSU-rRNA; IBA:GO_Central.
GO:1904872; P:regulation of telomerase RNA localization to Cajal body; IMP:BHF-UCL.
GO:1904874; P:positive regulation of telomerase RNA localization to Cajal body; IMP:BHF-UCL.
GO:1904911; P:negative regulation of establishment of RNA localization to telomere; IMP:BHF-UCL.
GO:1905216; P:positive regulation of RNA binding; IMP:CAFA.
GO:1905382; P:positive regulation of snRNA transcription by RNA polymerase II; ISS:UniProtKB.
GO:1905612; P:positive regulation of mRNA cap binding; IDA:ParkinsonsUK-UCL.
GO:1905618; P:positive regulation of miRNA mediated inhibition of translation; IDA:ParkinsonsUK-UCL.
GO:1905636; P:positive regulation of RNA polymerase II regulatory region sequence-specific DNA binding; IMP:ParkinsonsUK-UCL.
GO:1905662; P:negative regulation of telomerase RNA reverse transcriptase activity; IMP:BHF-UCL.
GO:1905663; P:positive regulation of telomerase RNA reverse transcriptase activity; ISS:BHF-UCL.

GO:1905869; P:negative regulation of 3'-UTR-mediated mRNA stabilization; IDA:UniProtKB.
GO:1905870; P:positive regulation of 3'-UTR-mediated mRNA stabilization; IMP:UniProtKB.
GO:1990074; P:polyuridylation-dependent mRNA catabolic process; ISS:UniProtKB.
GO:1990114; P:RNA polymerase II core complex assembly; IMP:UniProtKB.
GO:1990180; P:mitochondrial tRNA 3'-end processing; IDA:UniProtKB.
GO:1990247; F:N6-methyladenosine-containing RNA binding; IDA:UniProtKB.
GO:1990248; P:regulation of transcription from RNA polymerase II promoter in response to DNA damage; IDA:ARUK-UCL.
GO:1990261; P:pre-mRNA catabolic process; IMP:UniProtKB.
GO:1990269; F:RNA polymerase II C-terminal domain phosphoserine binding; IDA:UniProtKB.
GO:1990280; P:RNA localization to chromatin; ISS:UniProtKB.
GO:1990428; P:miRNA transport; ISS:BHF-UCL.
GO:1990440; P:positive regulation of transcription from RNA polymerase II promoter in response to endoplasmic reticulum stress; TAS:ParkinsonsUK-UCL.
GO:1990441; P:negative regulation of transcription from RNA polymerase II promoter in response to endoplasmic reticulum stress; IMP:ParkinsonsUK-UCL.
GO:1990481; P:mRNA pseudouridine synthesis; IMP:UniProtKB.
GO:1990511; P:piRNA biosynthetic process; ISS:UniProtKB.
GO:1990715; F:mRNA CDS binding; IEA:Ensembl.
GO:1990744; P:primary miRNA methylation; IDA:UniProtKB.
GO:1990817; F:RNA adenylyltransferase activity; IEA:InterPro.
GO:1990825; F:sequence-specific mRNA binding; ISS:UniProtKB.
GO:1990883; F:rRNA cytidine N-acetyltransferase activity; IBA:GO_Central.
GO:1990930; F:RNA N1-methyladenosine dioxygenase activity; IDA:UniProtKB.
GO:1990931; F:RNA N6-methyladenosine dioxygenase activity; IDA:UniProtKB.
GO:1990932; F:5.8S rRNA binding; IEA:Ensembl.
GO:1990968; P:modulation by host of RNA binding by virus; IMP:ParkinsonsUK-UCL.
GO:1990969; P:modulation by host of viral RNA-binding transcription factor activity; IGI:ParkinsonsUK-UCL.
GO:1990983; P:tRNA demethylation; IDA:UniProtKB.
GO:1990984; F:tRNA demethylase activity; IDA:UniProtKB.
GO:2000232; P:regulation of rRNA processing; IDA:UniProtKB.
GO:2000233; P:negative regulation of rRNA processing; ISS:UniProtKB.
GO:2000234; P:positive regulation of rRNA processing; IMP:UniProtKB.
GO:2000623; P:negative regulation of nuclear-transcribed mRNA catabolic process, nonsense-mediated decay; IMP:UniProtKB.
GO:2000626; P:negative regulation of miRNA catabolic process; IDA:UniProtKB.
GO:2000627; P:positive regulation of miRNA catabolic process; IDA:UniProtKB.
GO:2000628; P:regulation of miRNA metabolic process; ISS:UniProtKB.
GO:2000630; P:positive regulation of miRNA metabolic process; IMP:BHF-UCL.
GO:2000632; P:negative regulation of pre-miRNA processing; IDA:UniProtKB.
GO:2000637; P:positive regulation of gene silencing by miRNA; IMP:UniProtKB.
GO:2000721; P:positive regulation of transcription from RNA polymerase II promoter involved in smooth muscle cell differentiation; IEA:Ensembl.
GO:2000730; P:regulation of termination of RNA polymerase I transcription; IEA:Ensembl.
GO:2000763; P:positive regulation of transcription from RNA polymerase II promoter involved in norepinephrine biosynthetic process; ISS:BHF-UCL.
GO:2000805; P:negative regulation of termination of RNA polymerase II transcription, poly(A)-coupled; IDA:UniProtKB.
GO:2000806; P:positive regulation of termination of RNA polymerase II transcription, poly(A)-coupled; IMP:UniProtKB.
GO:2000815; P:regulation of mRNA stability involved in response to oxidative stress; IBA:GO_Central.
GO:2000820; P:negative regulation of transcription from RNA polymerase II promoter involved in smooth muscle cell differentiation; ISS:BHF-UCL.
GO:2000827; P:mitochondrial RNA surveillance; IMP:UniProtKB.
GO:2001141; P:regulation of RNA biosynthetic process; ISS:ARUK-UCL.
GO:2001165; P:positive regulation of phosphorylation of RNA polymerase II C-terminal domain serine 2 residues; IMP:CACAO.